CHAPTER 5

Theoretical Insights Into Chain Transfer Reactions of Acrylates

Masoud Soroush[1] **and Andrew M. Rappe**[2]

[1]*Department of Chemical and Biological Engineering, Drexel University, Philadelphia, PA, United States* [2]*Department of Chemistry, University of Pennsylvania, Philadelphia, PA, United States*

5.1 Introduction

Alkyl acrylates are widely used as primary binders in coating formulations for the automobile industry [1–5]. The basic nature of acrylic resins and the processing plants producing the resins have changed considerably over the past decades as a result of environmental limits on the resins' allowable volatile organic contents (VOCs) [6–8]. High temperature ($>100^{\circ}C$) polymerization, which allows for the production of high-solids low–molecular weight resins, has mostly replaced conventional (low-temperature) polymerization, which produces low-solids high molecular–weight resins [1,9,10]. It has been reported [1,2,11–15] that at higher temperatures, secondary reactions, such as spontaneous initiation, backbiting, β-scission, and chain transfer to monomer and polymer, should be accounted for in describing polymerization of alkyl acrylates. The production of alkyl acrylate polymers with polydispersity indices of 1.5–2.2 [14,16] at high temperatures indicated that various types of chain transfer reactions occur at high rates at the high temperatures. Recent studies using quantum chemical calculations [11,12] and matrix-assisted laser desorption ionization (MALDI) [16] showed that monomer self-initiation is a likely mechanism of initiation in the spontaneous thermal polymerization of alkyl acrylates. Monoradicals (a monomeric monoradical (MMR), $M_1^{\bullet}$, and a dimeric monoradical, $M_2^{\bullet}$) generated by the self-initiation mechanism [11,12] are shown in Fig. 5.1.

A better understanding of the mechanisms of chain transfer reactions is important for developing more efficient high-temperature polymerization processes. Previous studies of thermally self-initiated polymerization of methyl acrylate (MA), ethyl acrylate (EA), and *n*-butyl acrylate (*n*BA) using electrospray ionization–Fourier transform mass spectrometry (ESI-FTMS) [15] and MALDI [16] showed abundant polymer chains with end groups formed by chain transfer reactions. Nuclear magnetic resonance (NMR) analysis of these polymers indicated the possible presence of end groups from chain transfer to monomer

Computational Quantum Chemistry.
DOI: https://doi.org/10.1016/B978-0-12-815983-5.00005-2

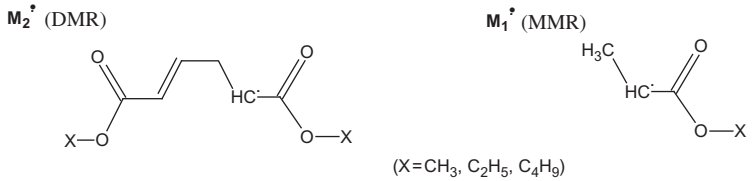

Figure 5.1
Two types of monoradicals generated by thermal self-initiation of alkyl acrylates, a monomeric monoradical (MMR) and a dimeric monoradical (DMR). *Reprinted with permission from N. Moghadam, S. Liu, S. Srinivasan, M.C. Grady, M. Soroush, A.M. Rappe, Computational study of chain transfer to monomer reactions in high-temperature polymerization of alkyl acrylates, J. Phys. Chem. A117 (2013) 2605–2618. Copyright 2013 American Chemical Society.*

(CTM) reactions at various temperatures (100–180°C) [15]. Chain transfer to solvent, monomer, and agent reactions terminate growing chains and start new growing chains that have no or one monomer unit. They are chain terminating reactions that do not affect the total number of free radicals in the reaction mixture. They lower dead polymer average molecular weights [17,18] and thus strongly influence the molecular weight distribution of dead polymer chains [19–22]. Intramolecular chain transfer to polymer (backbiting) reactions allow for the formation of midchain radicals that provide reaction sites for short-chain branching and β-scission. β-Scission reactions are of great interest in resin and coating manufacturing, because without the involvement of any other molecules, they divide a live polymer chain into a shorter live polymer chain and a shorter dead polymer chain with a terminal double bond, thus lowering dead polymer average molecular weights without altering the total number of free radicals in the reaction mixture. The dead polymer chain with a terminal double bond can then act as a macromonomer; that is, it can participate in a propagation or crosslinking reaction. Unlike chain transfer and β-scission reactions, termination by combination and disproportionation reactions form dead polymer chains by consuming two live polymer chains, thus lowering the total number of free radicals in the reaction mixture. The polymerization rate depends directly on the total number of free radicals in the reaction mixture. Accordingly, those reactions that terminate live chains without decreasing the total number of free radicals, allow for polymerization to take place at a sustained rate, with less conventional thermal initiators.

Controlled radical polymerization processes, such as nitroxide-mediated polymerization, atom transfer radical polymerization, and reversible addition-fragmentation chain transfer, can also benefit from a better understanding of chain transfer reactions. These processes involve the use of agents that regulate the growth of propagating chains, leading to the formation of uniform chain-length polymers [23–29]. It has been reported that in thermal polymerization of alkyl acrylates, in the absence of these agents, uniform chain length polymers can be synthesized [14]. This suggests that some chain transfer reactions are capable

of regulating polymer chain length. Therefore, a good understanding of the underlying chain transfer mechanisms help develop self-controlled thermal polymerization processes.

Experimental studies of the chain transfer reactions provided a general description of each chain transfer reaction as one involving a live polymer chain with a transfer agent (monomer, polymer, solvent, initiator, or chain transfer agent), without conclusively suggesting any reaction mechanisms [30,31]. Pulsed-laser polymerization/size exclusion chromatography (PLP/SEC) experiments were carried out at low and high temperatures to determine chain transfer and radical propagation rate coefficients of acrylates [32–34]. While yielding reliable results at lower temperatures, the experiments provided broad or featureless molecular-weight distributions at temperatures above 30°C [35–37]. CTM [32,33,35] and chain transfer to polymer (specifically backbiting) [36,38,39] were identified as the main causes of the broad or featureless molecular-weight distributions.

Reaction rate constants in high-temperature polymerization of alkyl acrylates have typically been estimated from polymer sample measurements, such as monomer conversion and average molecular weights, using macroscopic-scale mechanistic first-principles mathematical models [2,40–42]. The reliability of these estimates depends on the validity of the postulated reaction mechanisms, kinetics, and the certainty of the measurements. Furthermore, this type of modeling is incapable of determining reaction mechanisms conclusively. The rate constants of CTM reactions in methyl methacrylate (MMA), styrene, and α-methylstyrene polymerization have been determined with little difficulty [20]. Maeder and Gilbert [22] estimated the rate constant of CTM reactions in emulsion polymerization of *n*BA from polymer molecular-weight distributions. CTM via hydrogen abstraction by tertiary poly*n*BA live chains from *n*BA molecules was reported [19,43,44]. However, CTM rate coefficients of acrylates are difficult to estimate reliably, due to large uncertainties in experimental measurements [44] and the presence of trace impurities that can act as chain transfer agents [22,45,46].

Computational quantum chemistry has provided invaluable additional information on chain transfer reactions by evaluating all likely chain transfer mechanisms, revealing the most likely mechanisms and predicting reaction kinetic parameters [47–51]. An objective of this chapter is to put these theoretical advances into perspective by pointing to new knowledge that was not obtainable via experimental studies but was gained from the theoretical investigations.

The organization of the rest of this chapter is as follows: Section 5.2 deals with chain transfer to monomer reactions. Section 5.3 concentrates on intermolecular chain transfer to polymer reactions, and Section 5.4 on chain transfer to solvent (CTS) reactions. Section 5.5 deals with backbiting (intramolecular chain transfer to polymer) and β-scission reactions. Section 5.6 discusses challenges in theoretical studies of reactions in solutions. Finally, the chapter ends with concluding remarks.

5.2 Chain Transfer to Monomer Reactions

In a CTM reaction, a live polymer chain reacts with a monomer molecule, generating a one-monomer unit live chain and a dead polymer chain. Accordingly, these reactions lower dead polymer average molecular weights [17,18] and strongly influence the molecular-weight distribution of dead polymer chains [19–22]. Other chain-terminating reactions, such as termination by combination and disproportionation, however, generate higher molecular-weight polymers compared to CTM reactions. While CTM reactions have been known for decades, little was known about the exact CTM mechanisms in homopolymerization of alkyl acrylates; only a general description of a chain transfer reaction was available as a reaction of a live polymer chain with a monomer, without conclusively knowing the most likely reaction mechanisms, the exact location of the hydrogen abstraction, or transfer in the molecules involved [30,52].

This section discusses advances made through theoretical investigations of mechanisms of CTM in homopolymerization of MA, EA, and *n*BA using computational quantum chemistry. The theoretical investigations led to the prediction of energy barriers and rate coefficients of the reactions involved in most likely mechanisms. These studies also examined the effects of live polymer chain length, the type of monoradical that initiates the live polymer chain, and the influence of live polymer chain radical type (tertiary vs. secondary) on the kinetics of CTM reactions.

5.2.1 Prior Experimental Knowledge

Experimental studies of the polymerization of MA, EA, and *n*BA using ESI-FTMS [14] and MALDI [16] showed abundant polymer chains with end groups formed by chain transfer reactions. NMR analysis of these polymers indicated the possible presence of end groups from CTM reactions at various temperatures (100–180°C) [14]. PLP/SEC experiments carried out at low and high temperatures were used to determine chain transfer and radical propagation rate coefficients of acrylates [32–34]. While yielding reliable results at lower temperatures, the experiments provided broad or featureless molecular-weight distributions at temperatures above 30°C [35–37]. CTM [32,33,35] and chain transfer to polymer (CTP) (specifically backbiting) [36,38,39] reactions were identified as the main causes of the broad or featureless molecular-weight distributions.

Rate coefficients of CTM reactions in MMA, styrene, and α-methylstyrene polymerization were determined [20,42]. Maeder and Gilbert [22] estimated rate coefficients of CTM reactions in emulsion polymerization of *n*BA from polymer molecular weight distributions. CTM via hydrogen abstraction by tertiary poly*n*BA live chains were reported [19,43,44]. However, large uncertainties in experimental measurements and the presence of trace

quantities of impurities that can act as chain transfer agents were blamed for large variations in estimates of CTM rate coefficients of acrylates [22,43,45,46].

Before the computational quantum chemistry studies, presented in the next section, only a general description of a CTM reaction was available; that is, CTM was known as a reaction of a live polymer chain with a monomer molecule, leading to the formation of a dead polymer chain and a one-monomer unit live polymer chain, without conclusively knowing the reaction mechanism(s) [30,31].

5.2.2 Knowledge Gained Using Quantum Chemical Calculations

Computational quantum chemistry has been used to study mechanisms of chain transfer from short live polymer chains. Moghadam et al. [51] studied chain transfer from the two two-monomer unit live chains: (1) the dimeric monoradical (DMR) $M_2^{\bullet}$, and (2) the two-monomer unit live polymer chain generated by the propagation of the MMR $M_1^{\bullet}$, shown in Fig. 5.1. The short live polymer chains (with two monomer units) were considered in the theoretical studies, because of (A) the exponential rise of the computation cost of simulating a polymer chain with the number of monomer units of the polymer chain, and (B) the well-established understanding that monomer units of a polymer chain beyond the penultimate unit have little effect on polymerization reaction rates.

5.2.2.1 Mechanisms of chain transfer from $M_2^{\bullet}$ to monomer

5.2.2.1.1 Methyl acrylate

Moghadam et al. [51] studied the four CTM mechanisms involving $M_2^{\bullet}$ radical of MA shown in Fig. 5.2. These mechanisms are: (1) MA-1: abstraction of a methyl hydrogen atom from a monomer molecule by the radical; (2) MA-2: abstraction of a β-hydrogen atom a monomer molecule by the radical; (3) MA-3: abstraction of an α-hydrogen atom from a monomer molecule by the radical; and (4) MA-4: transfer of a β-hydrogen of the saturated monomer unit of the live polymer chain to the β-carbon atom of a monomer molecule. Using different levels of theory, MA-1 was found to be the most kinetically favorable mechanism, as MA-2 and MA-3 mechanisms have higher activation energies. This agrees with the fact that the bond-dissociation energy of a methyl hydrogen is lower than that of an α- or β-hydrogen [51].

5.2.2.1.2 Ethyl acrylate

Moghadam et al. [51] studied the two CTM mechanisms, shown in Fig. 5.3, in which $M_2^{\bullet}$ abstracts a hydrogen from a carbon atom of the ethyl group of an EA molecule [51] (EA-1: abstraction of a hydrogen from the methylene bridge (methanediyl group) of a monomer molecule, and EA-2: abstraction of a hydrogen from the methyl group of a monomer

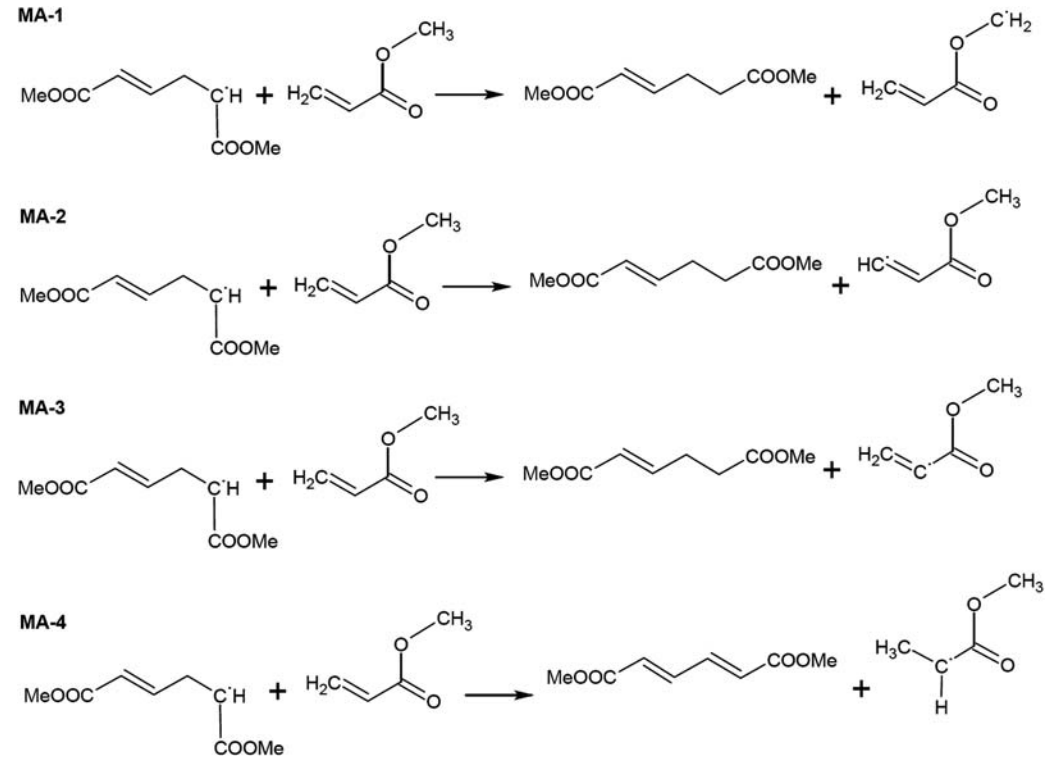

Figure 5.2

Possible chain transfer from $M_2^{\bullet}$ to monomer reactions for MA. *Reprinted with permission from N. Moghadam, S. Liu, S. Srinivasan, M.C. Grady, M. Soroush, A.M. Rappe, Computational study of chain transfer to monomer reactions in high-temperature polymerization of alkyl acrylates, J. Phys. Chem. A117 (2013) 2605−2618. Copyright 2013 American Chemical Society.*

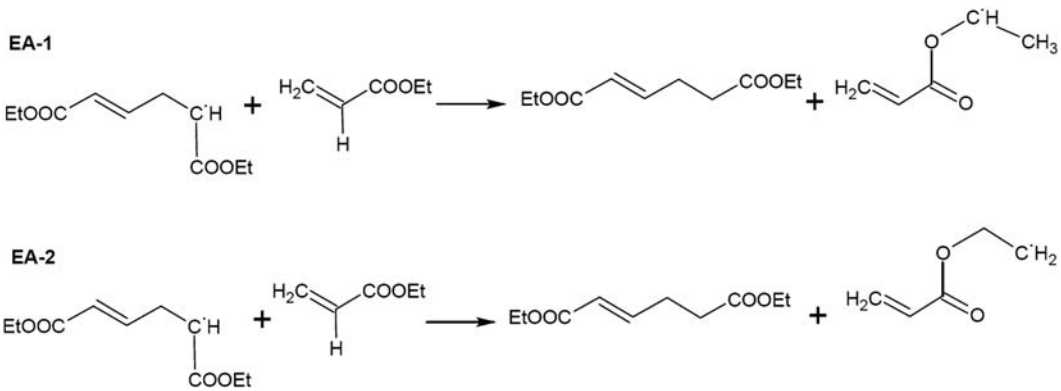

Figure 5.3

Possible chain transfer from $M_2^{\bullet}$ to monomer reactions for EA. *Reprinted with permission from N. Moghadam, S. Liu, S. Srinivasan, M.C. Grady, M. Soroush, A.M. Rappe, Computational study of chain transfer to monomer reactions in high-temperature polymerization of alkyl acrylates, J. Phys. Chem. A 117 (2013) 2605−2618. Copyright 2013 American Chemical Society.*

molecule). The abstraction of a β- or α-hydrogen from a monomer molecule by $M_2^{\bullet}$ was not studied, as these reactions in MA had already been shown to have higher energy barriers. The barrier of the EA-1 mechanism was found to be lower than that of the EA-2 mechanism. The rate constants and barriers were found to depend more on the type of density functional theory (DFT) functional that was used, than on the type of basis set, which agrees with findings for MA [51]. These results indicated that monomer chain transfer in thermal polymerization of EA most likely occurs via the abstraction of a hydrogen from the methyl group of an EA molecule.

5.2.2.1.3 *n*-Butyl acrylate

For *n*BA, Moghadam et al. [51] studied the four CTM mechanisms, shown in Fig. 5.4, involving the $M_2^{\bullet}$ radical. These mechanisms are: (1) *n*-BA-1, *n*-BA-2 and *n*-BA-3:

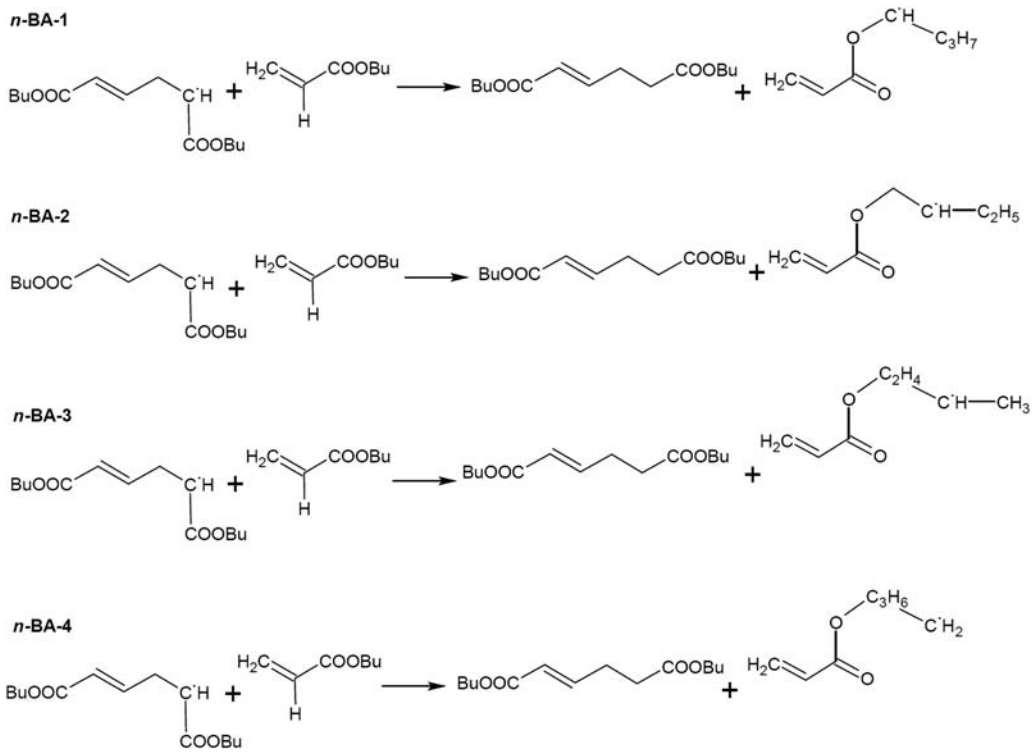

Figure 5.4

Possible chain transfer from $M_2^{\bullet}$ to monomer reactions for *n*BA. *Reprinted with permission from N. Moghadam, S. Liu, S. Srinivasan, M.C. Grady, M. Soroush, A.M. Rappe, Computational study of chain transfer to monomer reactions in high-temperature polymerization of alkyl acrylates, J. Phys. Chem. A 117 (2013) 2605−2618. Copyright 2013 American Chemical Society.*

abstraction of a hydrogen from each of the three methylene bridges (methanediyl groups) of a monomer molecule by the radical, and (2) *n*-BA-4: abstraction of a methyl hydrogen from a monomer molecule by the radical. Different levels of theory mostly predicted that the rate coefficient of *n*-BA-1 is higher than those of *n*-BA-2, *n*-BA-3 and *n*-BA-4. The activation energy and rate coefficient of hydrogen abstraction from the methanediyl group adjacent to the ester oxygen (*n*-BA-1) calculated using M06-2X/6-31G(*d,p*) were found to be quite comparable to experimental values [19]; that is, 31 kJ mol^{-1} versus 31 kJ mol^{-1} (theoretical vs. experimental [19,22]) and 0.5 L mol^{-1} s^{-1} versus 0.6 L mol^{-1} s^{-1} (theoretical vs. experimental [19,22]). The abstraction of a hydrogen atom from the methanediyl group adjacent to the methyl group was found to have the highest activation energy among the three methanediyl hydrogen abstraction reactions [51].

The activation energy for the most favorable CTM mechanism in MA (MA-1) was found to be much higher (by $\sim$20 kJ mol^{-1}) than those for the most favorable ones in EA (EA-1) and *n*BA (*n*-BA-1) [51]. This indicates that the length of the side-chain influences the height of the barrier.

Using different methods (B3LYP and X3LYP) and several basis sets (6−31G(*d*), 6−31G (*d,p*), 6−311G(*d*), and 6−311G(*d,p*)), C-NMR chemical shifts of the dead polymer chains formed by the most probable CTM mechanisms (MA-1, EA-1, *n*-BA-1) were calculated [51]. Similar values for the chemical shifts were obtained using the functionals. The calculated NMR chemical shifts for the dead polymer chains generated via the MA-1, EA-1, and *n*-BA-1 mechanisms [51] were found to be comparable with experimental values reported for spontaneous polymerization of *n*BA [14,53]. This agreement suggests that the mechanisms identified via quantum chemical calculations are likely occurring in thermal polymerization of alkyl acrylates. No experimental result in spontaneous polymerization was found to be similar to the calculated chemical shifts of the product generated by the MA-4 mechanism (Fig. 5.2), implying that the MA-4 mechanism is very unlikely to occur. The computational quantum chemistry studies also indicated that the abstraction of a hydrogen via the MA-1, EA-1 and *n*-BA-1 mechanisms are also most thermodynamically favorable, in addition to being most kinetically favorable.

5.2.2.2 Mechanisms of chain transfer from $M_1^{\bullet}$-initiated dimeric monoradical to monomer

The CTM reactions of a two-monomer unit live polymer chain initiated by $M_1^{\bullet}$ (MA-1, EA-1 and *n*-BA-1 in Fig. 5.5) were investigated using B3LYP, X3LYP and M06-2X functionals [51]. These results revealed that CTM reactions of $M_2^{\bullet}$ and the $M_1^{\bullet}$-initiated dimeric monoradical have similar activation energies and rate constants, which indicates that the type of initiating radicals of live polymer chains has very little effect on the rates of the CTM reactions.

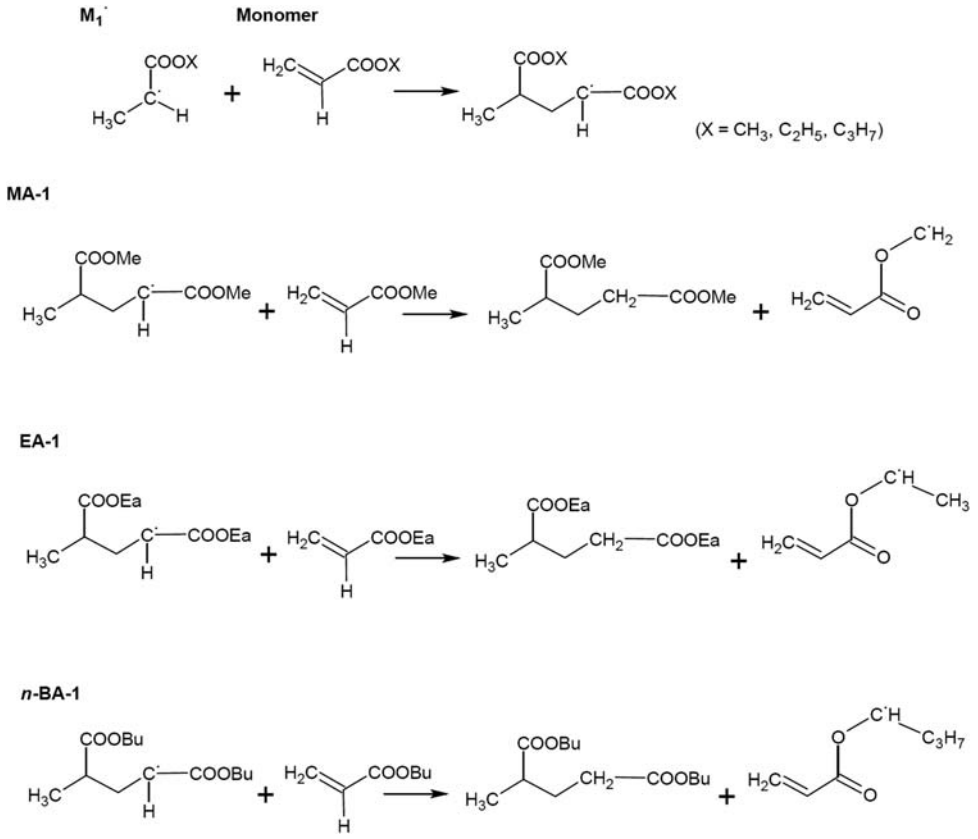

Figure 5.5

The most probable mechanisms for CTM reactions involving a two-monomer unit live chain initiated by $M_1^{\bullet}$. *Reprinted with permission from N. Moghadam, S. Liu, S. Srinivasan, M.C. Grady, M. Soroush, A.M. Rappe, Computational study of chain transfer to monomer reactions in high-temperature polymerization of alkyl acrylates, J. Phys. Chem. A 117 (2013) 2605−2618. Copyright 2013 American Chemical Society.*

5.2.2.3 Effect of live polymer chain length

Moghadam et al. [51] studied theoretically chain transfer from a three-monomer unit live chain initiated by $M_2^{\bullet}$ to a monomer molecule, via the MA-1, EA-1 and *n*-BA-1 mechanisms, shown in Fig. 5.6, to understand the effect of live polymer chain length on the kinetics of CTM. It was observed that the transition-state geometries of three-monomer unit live chains are similar to those of two-monomer unit live chains discussed in Section 5.2.2.1. This implies that the end-substituent group does not significantly affect the geometry of the reaction center. Activation energies of the CTM reactions calculated using B3LYP/6−31G(*d*) were found to vary very little with the length of the polymer chain [51]. However, M06-2X/6−31G(*d*,*p*) did show an increase in the energy barrier for *n*-BA-1 with

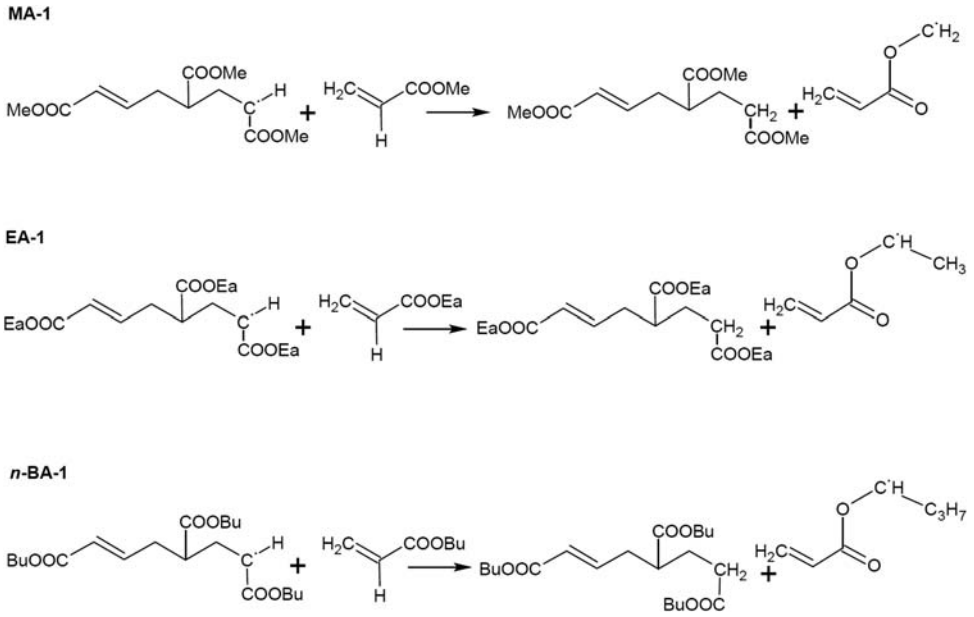

Figure 5.6

The most probable mechanisms for CTM reactions involving a three-monomer unit live chain initiated by $M_2^{\bullet}$. *Reprinted with permission from N. Moghadam, S. Liu, S. Srinivasan, M.C. Grady, M. Soroush, A.M. Rappe, Computational study of chain transfer to monomer reactions in high-temperature polymerization of alkyl acrylates, J. Phys. Chem. A 117 (2013) 2605–2618. Copyright 2013 American Chemical Society.*

the length of the live chain. The hybrid meta functional M06-2X is more likely to describe chain length effects in CTM reactions for alkyl acrylates more accurately, especially for the large systems (e.g. *n*BA).

5.2.2.4 Effect of live-polymer radical type on CTM

Moghadam et al. [51] theoretically compared chain transfer from secondary and tertiary radicals to a monomer molecule. They considered the two CTM reactions shown in Fig. 5.7. The CTM reaction of an $M_1^{\bullet}$-initiated three-monomer unit live tertiary radical, denoted by $Q_3^{\bullet}$; and the CTM reaction of an $M_1^{\bullet}$-initiated three-monomer unit secondary radical, denoted by $P_3^{\bullet}$. Calculated energy barriers and rate constants of these two mechanisms indicated that the activation energy of hydrogen abstraction by a tertiary radical from a monomer molecule is higher than that of hydrogen abstraction by a secondary radical [51]. This implies that a tertiary-radical carbon is more likely to participate in (1) a propagation reaction (form a covalent bond with the β-carbon atom of a monomer molecule, creating a chain branch), or (2) a β-scission reaction, than in a CTM reaction (abstracting an hydrogen from a monomer molecule). This finding agrees with previous reports [13,14] that showed the formation of chain branches on tertiary radicals using NMR and mass spectrometry.

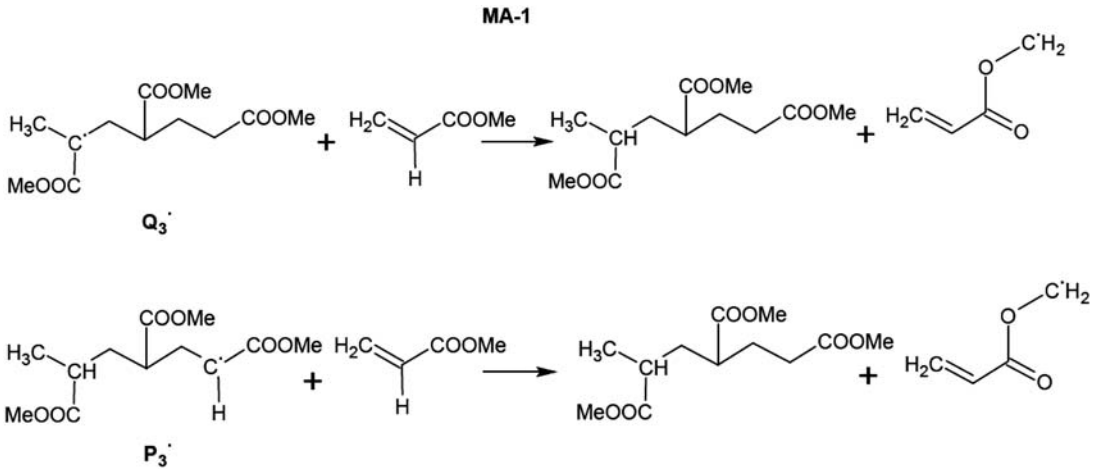

Figure 5.7
CTM reactions involving the live chains $Q_3^{\bullet}$ and $P_3^{\bullet}$. *Reprinted with permission from N. Moghadam, S. Liu, S. Srinivasan, M.C. Grady, M. Soroush, A.M. Rappe, Computational study of chain transfer to monomer reactions in high-temperature polymerization of alkyl acrylates, J. Phys. Chem. A 117 (2013) 2605–2618. Copyright 2013 American Chemical Society.*

5.2.3 CTM Summary

Computational quantum chemistry indicated that the abstraction of a methanediyl hydrogen by a live polymer chain in EA and *n*BA, and a methyl group hydrogen in MA are the most likely mechanisms for CTM reactions [51]. In particular, in CTM reactions of alkyl acrylates, a live polymer chain most likely abstracts an hydrogen atom from the alkyl side-chain carbon atom adjacent to the ester oxygen of a monomer molecule. The reaction kinetic parameters calculated using M06-2X/6−31G(*d,p*) were found to be closest to those estimated from polymer sample measurement. Theoretically predicted NMR chemical shifts of the dead polymer chains formed by the MA-1, EA-1 and *n*-BA-1 reactions were found to be comparable to those from polymer sample analyses, which confirms that the chain transfer mechanisms suggested by computational quantum chemistry actually occur in the homopolymerization of MA, EA, and nBA. Calculations using the B3LYP/6−31G(*d*) functional indicated that the polymer chain length had little effect on the activation energies and rate constants of CTM reactions. However, calculations using M06-2X/6−31G(*d,p*) showed otherwise. All three MA, EA, and nBA live polymer chains initiated by $M_2^{\bullet}$ and those initiated by $M_1^{\bullet}$ showed similar hydrogen abstraction abilities, which is indicative of the weak influence of self-initiating species on CTM reactions. A tertiary radical carbon has much less tendency to abstract a hydrogen than a secondary radical.

5.3 Intermolecular Chain Transfer to Polymer Reactions

There are two types of CTP reactions: intramolecular and intermolecular CTP reactions. In intramolecular chain transfer reactions (backbiting), a secondary radical (live chain)

abstracts a hydrogen atom from its backbone, producing a midchain radical [53–56]. In this case, the live chain stops growing from its head but starts growing from a carbon atom further inside the chain. In intermolecular chain transfer reactions, however, a live polymer chain abstracts a hydrogen atom from a dead polymer chain [15,53], stopping further growth of the live polymer chain and initiating a new live chain. While intermolecular CTP reactions have been known for decades, little was known about the exact intermolecular CTP mechanisms in the homopolymerization of alkyl acrylates. Only a general description of a chain transfer reaction was available as a reaction of a live polymer chain with a dead polymer chain, without conclusively specifying the most likely reaction mechanisms.

This chapter puts into perspective advances made through computational quantum chemistry studies of mechanisms of intermolecular CTP in homopolymerization of MA, EA, and *n*BA [50]. These studies predicted energy barriers and rate coefficients of the reactions involved in the postulated mechanisms. The effect of live polymer chain length, the type of the monoradical that initiated the live polymer chain, the structure of the dead polymer chain, and the type of live polymer chain radical (tertiary vs secondary) on the kinetics of the CTP reactions were investigated. In this section, by CTP we mean intermolecular CTP, unless CTP is denoted by intramolecular.

5.3.1 Prior Experimental Knowledge

It was reported that, at low polymer concentrations, intramolecular CTP is dominant [53], but at high polymer concentrations intermolecular CTP is dominant [10,14,15,53,57–59]. New radicals generated by CTP reactions can then propagate to form branches or terminate by coupling with other propagating radicals [15]. The contribution of CTP reactions to branching was explored for controlled radical polymerization [60] and conventional free-radical polymerization of *n*BA, and the level of branching as a function of transient lifetime was studied [57,59]. The effects of midchain radicals, formed by intermolecular and intramolecular CTP reactions, on *n*BA termination reactions at high-temperatures were studied experimentally and compared with those of secondary radicals [61]. Numerous experimental and theoretical investigations [38,39,45,53,62–74] revealed that CTP reactions can strongly impact the overall rate of polymerization.

Intermolecular and intramolecular CTP and β-scission reactions in thermal polymerization of *n*BA and *n*-butyl methacrylate were studied using NMR spectroscopy and electrospray ionization/Fourier transform mass spectroscopy (ESI/FTMS) [1,15,75]. NMR analysis of the polymers indicated the presence of end groups from CTP reactions at temperatures lower than 70°C [53,64,75]. Experimental studies showed the important role of intramolecular chain transfer and β-scission reactions in decreasing dead polymer average molecular weights and increasing polymerization rate [13,15,76,77]. Both NMR and ESI/FTMS analyses of samples from spontaneous (no thermal initiator added) high-temperature homopolymerization of EA and *n*BA showed that different branch points are generated

during the polymerization [14]. The NMR and ESI/FTMS analyses revealed the presence of branch points, indicating the propagation of mid-chain tertiary radicals [14] generated through CTP reactions. The kinetics of CTP reactions in alkyl acrylates were studied using PLP/SEC [34,76]. Molecular-weight distributions of PLP-generated polymers showed peak broadening at temperatures above 30°C, pointing to the occurrence of both intermolecular and intramolecular CTP reactions [64,78,79]. At temperatures above 30°C, intermolecular CTP reactions in free-radical polymerization of *n*BA [15,53] and 2-ethylhexyl acrylate [75] were also studied using NMR spectroscopy. While these analytical techniques were very useful in characterizing acrylate polymers generated from thermal free-radical polymerizations, by themselves they were incapable of conclusively identifying reaction mechanisms or estimating reaction kinetic parameters.

Macroscopic kinetic models were used extensively [2] to estimate the rate constants of initiation, propagation, chain transfer and termination reactions in free-radical polymerization of acrylates, from polymer sample measurements such as monomer conversion and average molecular weights [2,40]. However, the accuracy of these kinetic parameter estimates depends on the accuracy of the model structure and measurements used in the estimation. These models are also incapable of conclusively determining mechanisms and intermediate molecular species involved.

As CTP reactions affect the polymerization rate and the molecular weight distribution of the polymer product [53,75], a better understanding of CTP reactions has been of great interest in optimizing polymerization processes and polymer properties [9,15,80]. Prior to the use of computational quantum chemistry to study CTP reactions [49,50,76], it was uncertain which carbon atoms were most likely to donate hydrogen atoms during CTP reactions.

5.3.2 Knowledge Gained Using Quantum Chemical Calculations

This section presents some of the advances made in better understanding mechanisms of CTP reactions in free-radical polymerization of alkyl acrylates (MA, EA, *n*BA) using DFT calculations [50]. Since there was only one unpaired spin in the systems that was considered, restricted open-shell wave functions were used in the calculations. Energy barriers were calculated and the molecular geometries of reactants, products, and transition states were optimized using the B3LYP functional. X3LYP and M06-2X functionals [81–83] were then applied to validate the calculated results. Four different basis sets (6−31G(*d*), 6−31G(*d,p*), 6−311G(*d*), and 6−311G(*d,p*)) were used with each of these functionals. Reactants and transition states were validated by performing Hessian calculations. NMR spectra of dead polymers generated by CTP mechanisms were calculated using functionals (B3LYP, and X3LYP) and basis sets (6−31G(*d*), 6−31G(*d,p*), 6−311G (*d*), and 6−311G(*d,p*)). These calculated spectra were compared with experimental spectra reported for EA and *n*BA polymers [14,53]. Implicit solvent models, the integral equation formalism-polarizable continuum model (IEF-PCM) and the conductor-like screening model

(COSMO), were applied to account for solvent effects. Minimum-energy pathways for several reactions of interest were determined using intrinsic reaction coordinate (IRC) calculations. GAMESS was used for all calculations [84].

Three dead polymer structures formed by the three termination reactions shown in Fig. 5.8 were considered. The two-monomer unit dead polymer D1 is the product of the termination by coupling reaction of two $M_1^{\bullet}$ MMRs (Fig. 5.8A). The two-monomer unit dead polymer D2 is the product of hydrogen abstraction by the dimeric monoradical formed by $M_1^{\bullet}$ undergoing one propagation step (Fig. 5.8B). The three-monomer unit dead polymer D3 is the product of the termination by coupling reaction of the $M_1^{\bullet}$ MMR and the dimeric monoradical formed by $M_1^{\bullet}$ undergoing one propagation step (Fig. 5.8C).

5.3.2.1 Chain Transfer to Dead Polymer

Possible mechanisms of chain transfer from $M_2^{\bullet}$ (a dimeric monoradical) to D1 (a dimmer) for MA, EA, and *n*BA are shown in Figs. 5.9–5.11, respectively [50]. The energy

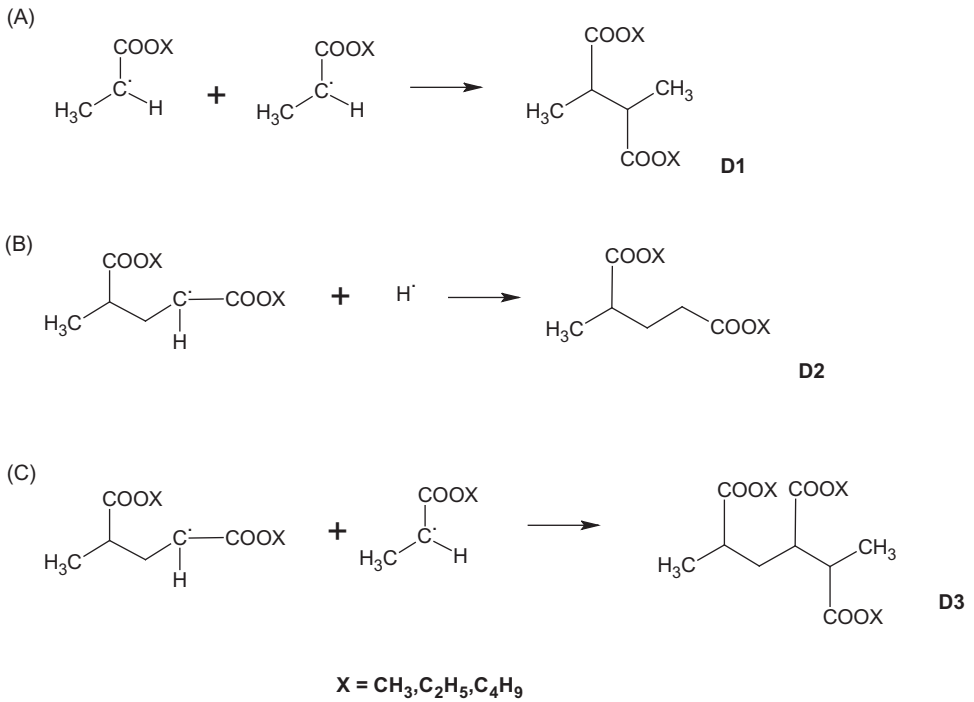

Figure 5.8

Dead polymer chains formed from (A) termination by coupling of two monomeric monoradicals (MMRs), (B) hydrogen abstraction by a dimeric monoradical, and (C) termination by coupling of a MMR and a dimeric monoradical. *Reprinted with permission from N. Moghadam, S. Liu, S. Srinivasan, M.C. Grady, A.M. Rappe, M. Soroush, Theoretical study of intermolecular chain transfer to polymer reactions of alkyl acrylates, Ind. Eng. Chem. Res. 54 (2015) 4148–4165. J. Phys. Chem. A 117 (2013) 2605–2618. Copyright 2013 American Chemical Society.*

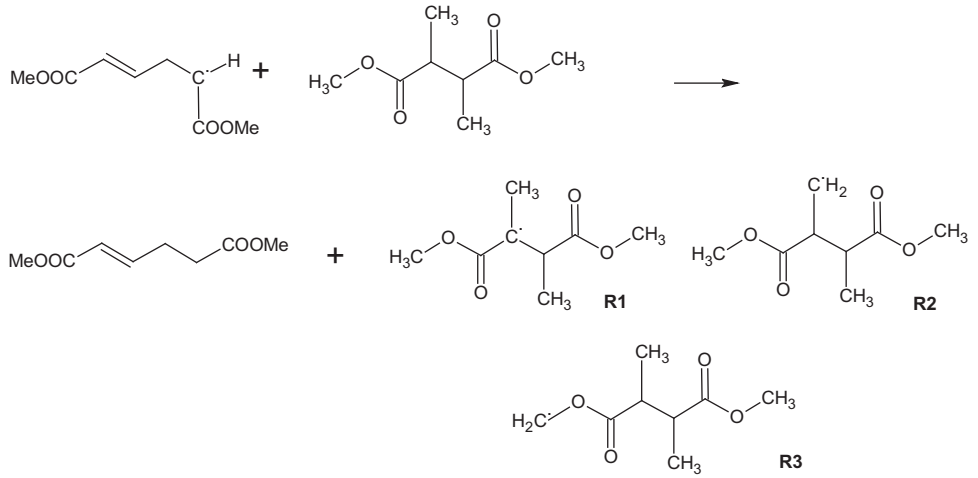

Figure 5.9

Possible chain transfer to polymer mechanisms for MA; MA2-D1-*i* mechanism produces the monoradical *Ri* (*i* = 1, 2, and 3). *Reprinted with permission from N. Moghadam, S. Liu, S. Srinivasan, M. C. Grady, A.M. Rappe, M. Soroush, Theoretical study of intermolecular chain transfer to polymer reactions of alkyl acrylates, Ind. Eng. Chem. Res. 54 (2015) 4148−4165. J. Phys. Chem. A 117 (2013) 2605−2618. Copyright 2013 American Chemical Society.*

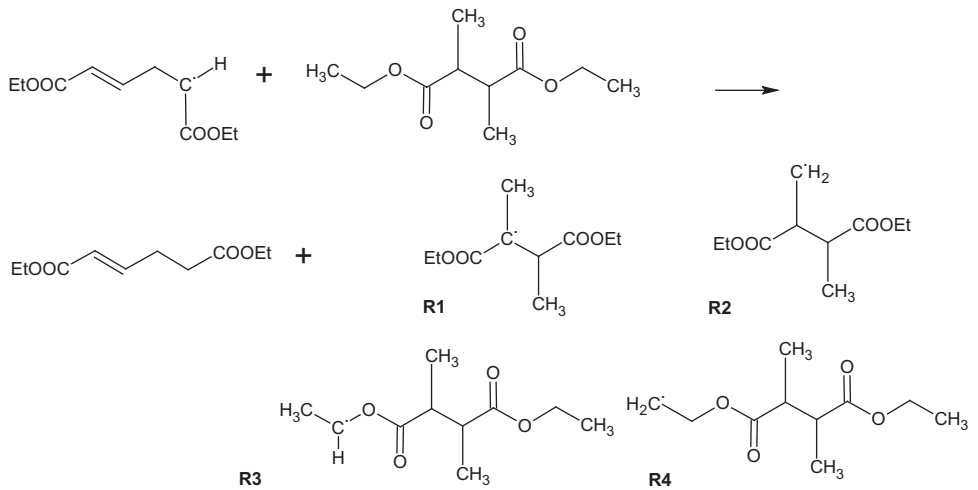

Figure 5.10

Possible chain transfer to polymer (CTP) mechanisms for EA; EA2-D1-*i* mechanism produces the monoradical *Ri* (*i* = 1, 2, 3, and 4). *Reprinted with permission from N. Moghadam, S. Liu, S. Srinivasan, M.C. Grady, A.M. Rappe, M. Soroush, Theoretical study of intermolecular chain transfer to polymer reactions of alkyl acrylates, Ind. Eng. Chem. Res. 54 (2015) 4148−4165. J. Phys. Chem. A 117 (2013) 2605−2618. Copyright 2013 American Chemical Society.*

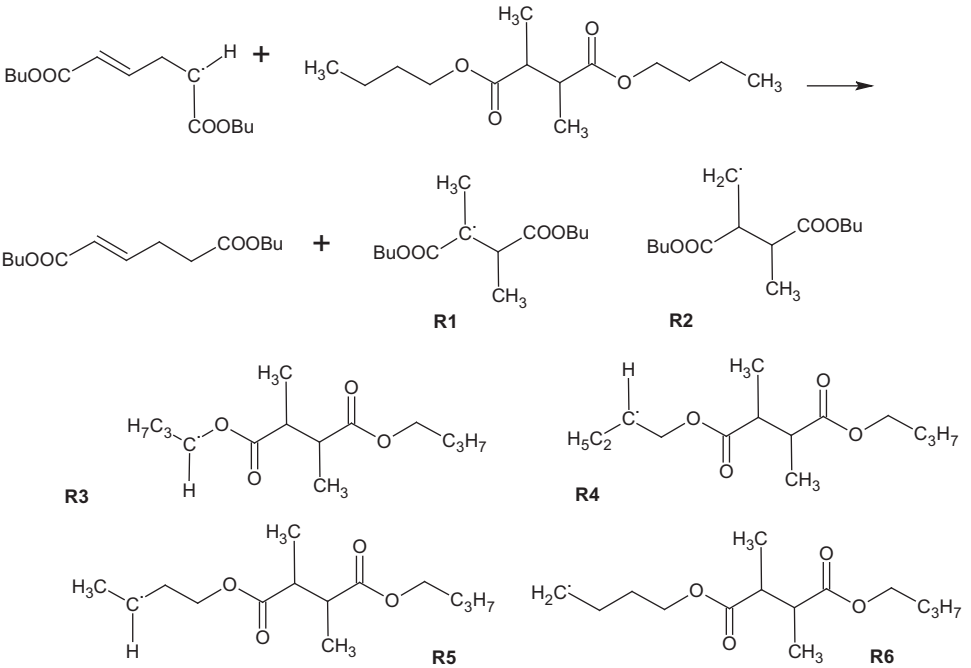

Figure 5.11

Possible chain transfer to polymer (CTP) mechanisms for *n*BA; *n*-BA2-D1-*i* mechanism produces the monoradical *Ri* ($i = 1, 2, 3, 4, 5$, and 6). *Reprinted with permission from N. Moghadam, S. Liu, S. Srinivasan, M.C. Grady, A.M. Rappe, M. Soroush, Theoretical study of intermolecular chain transfer to polymer reactions of alkyl acrylates, Ind. Eng. Chem. Res. 54 (2015) 4148–4165. J. Phys. Chem. A 117 (2013) 2605–2618. Copyright 2013 American Chemical Society.*

differences of optimized reactants and products involved in each of these mechanisms were calculated by applying B3LYP and X3LYP functionals and 6-31G(*d*), 6-31G(*d,p*), 6-311G (*d*) and 6-311G(*d,p*) basis sets. The results indicated that MA2-D1-1, EA2-D1-1, and *n*-BA2-D1-1 mechanisms (that form R1, a tertiary radical) are exothermic, whereas the other mechanisms are endothermic (Figs. 5.9–5.11). X2-D1-*i* denotes the abstraction of a hydrogen by the dimeric monoradical $M_2^{\bullet}$ from the dead polymer chain D1 to form the radical R*i* when the monomer is X. These findings make sense, as tertiary radicals are more stable than secondary radicals [85,86], increasing the likelihood of the MA2-D1-1, EA2-D1-1, and *n*-BA2-D1-1 mechanisms to occur.

The same functionals and basis sets were used to calculate the bond-dissociation energies of hydrogen atoms involved in the proposed mechanisms. These dissociation energies were found to agree with previous results [83] and that the bond-dissociation energies of tertiary hydrogen atoms (which are abstracted via MA2-D1-1, EA2-D1-1, and *n*-BA2-D1-1 mechanisms) are

about 50 kJ mol^{-1} lower than those of other hydrogen atoms of the dead polymers [50]. This suggested that a tertiary carbon atom has a higher tendency to donate a hydrogen.

5.3.2.1.1 Effect of the type of the radical that initiated a live methyl acrylate-polymer chain

The abstraction of a tertiary hydrogen from the dead polymer chain D1 by the dimeric monoradical formed by $M_1^{\bullet}$ undergoing one propagation step (MA1-D1-1, shown in Fig. 5.12) and by the dimeric monoradical $M_2^{\bullet}$ (MA2-D1-1, shown in Fig. 5.9) was compared, where the monoradicals $M_1^{\bullet}$ and $M_2^{\bullet}$ are shown in Fig. 5.1. The activation energies and rate constants of the MA2-D1-1 mechanism calculated using functionals B3LYP, X3LYP, and M06-2X, and several basis sets were found to be different by $\pm$ 10 kJ mol^{-1} and two orders of magnitude, respectively [50]. The kinetic and thermodynamic parameters predicted using the M06-2X functional were observed to be very different from those obtained with B3LYP and X3LYP. It is worth mentioning that M06-2X functional accounts for van der Waals (vdW) interactions [87,88]. B3LYP is a hybrid GGA functional, but M06-2X is a hybrid meta-GGA functional. The rate constant estimates calculated using M06-2X were found to be in good agreement with experimental values reported for CTM reactions of MA, EA, and *n*BA [51]. No significant change in activation energies or rate constants was observed when different basis sets were used. The type of radical that initiated a live chain was reported to have little or no effect on the CTP reactivity of the live chain [50].

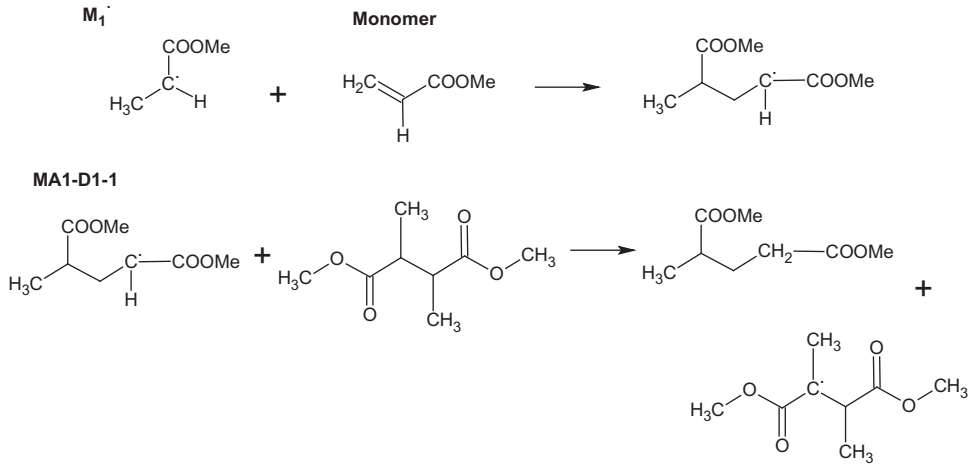

Figure 5.12

Most probable CTP mechanism involving two-MA-unit live chain initiated by $M_1^{\bullet}$. *Reprinted with permission from N. Moghadam, S. Liu, S. Srinivasan, M.C. Grady, A.M. Rappe M. Soroush, Theoretical study of intermolecular chain transfer to polymer reactions of alkyl acrylates, Ind. Eng. Chem. Res. 54 (2015) 4148–4165. J. Phys. Chem. A 117 (2013) 2605–2618. Copyright 2013 American Chemical Society.*

5.3.2.1.2 Chain transfer to polymer mechanisms for EA and *n*BA

The EA2-D1-1 (Fig. 5.10) and *n*-BA2-D1-1 (Fig. 5.11) CTP mechanisms that involve the abstraction of a tertiary hydrogen from the dead polymer chain D1 by the dimeric monoradical $M_2^{\bullet}$, was studied using B3LYP and X3LYP methods and 6−31G(*d*), 6−31G(*d,p*), 6−311G(*d*), and 6−311G(*d,p*)) basis sets [50]. The predicted activation energies and rate constants were found to be different by maximum 13 kJ mol^{-1} and two orders of magnitude, respectively. The performance of M06-2X with different basis sets was found to be more consistent: the calculated activation energies and the rate constants were different by 3 kJ mol and one order of magnitude. *n*-BA2-D1-1 was found to be the most probable mechanism of CTP, which is in agreement with previous studies [76]. The activation energy calculated using B3LYP (6−31G(*d,p*)) was $\sim$20 kJ mol^{-1} higher than a reported experimental value of 29 kJ mol^{-1} [76], and the rate constant was lower by about four orders of magnitude [76]. This indicates that the level of theory applied was adequate to accurately predict the mechanistic pathway and transition-state structures but not the quantitative reaction rate. This inadequacy was attributed to the limitation of the hybrid functionals and the use of the rigid rotor harmonic oscillator (RRHO) approximation. Although discrepancies between DFT-calculated and experimentally determined activation energies and frequency factors were reported in this study, other studies showed that DFT is a reliable approach for predicting rate constants in free-radical polymerization [48,51,54−56,89−91].

The kinetic parameters estimated for the most likely CTP mechanisms of MA, EA, and *n*BA (MA2-D1-1, EA2-D1-1, and *n*-BA2-D1-1) indicated that the end-substituent groups (methyl, ethyl, and butyl acrylate side chains) do not affect the kinetics of the CTP reaction in the alkyl acrylates [50]. This can be explained through the similarity of the most reactive sites involved in the CTP reaction of MA, EA, and *n*BA [47,51]. The pathways for the CTP mechanisms in the alkyl acrylates (MA2-D1-1, EA2-D1-1, and *n*-BA2-D1-1), determined through IRC calculations in the forward and backward directions started from transition-state structures for MA, EA, and *n*BA, showed the presence of concerted pathways [50].

5.3.2.1.3 Effect of the live polymer chain length

The effects of the length of a live polymer chain on the activation energies and the geometries of transition states of CTP reactions were explored for MA and EA. In particular, the abstraction of an hydrogen atom by a three or four monomer-unit live chain initiated by $M_2^{\bullet}$ from a dead polymer chain D1 was investigated for MA (Fig. 5.13) [50]. These studies showed that the rate constants of the two CTP reactions involving the three- and four-monomer unit live chains, MA2-D1-1(A) and MA2-D1-1(B), are different by at most two orders of magnitude, and the activation energies of these two reactions very little (at most by 4 kJ mol^{-1}) [50].

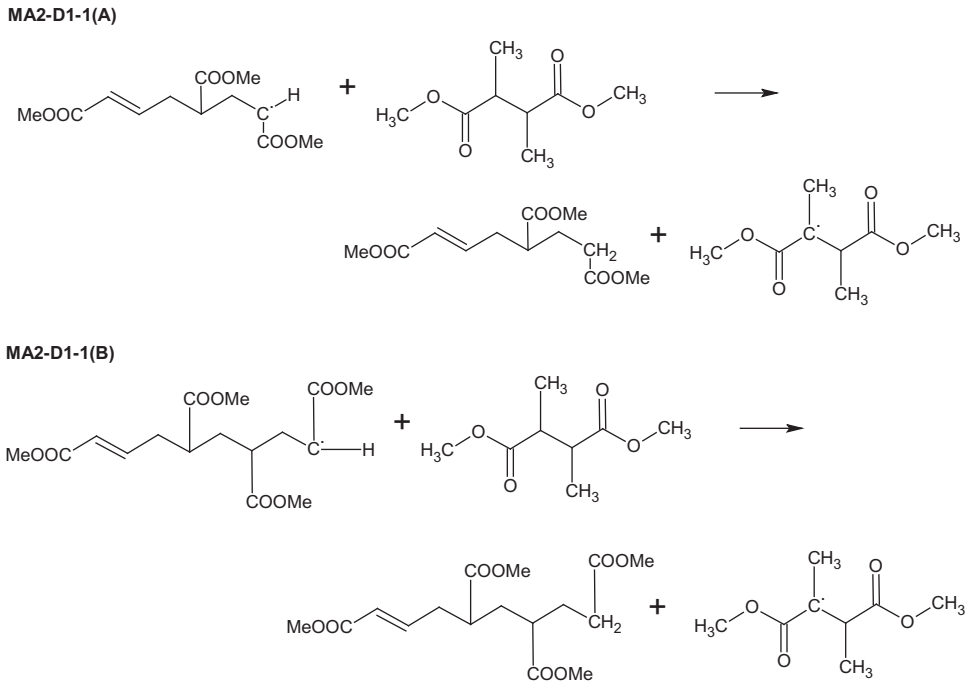

Figure 5.13

Most probable CTP mechanism involving a three [MA2-D1-1(A)] or four [MA2-D1-1(B)] MA-unit live chain initiated by $M_2^{\bullet}$. *Reprinted with permission from N. Moghadam, S. Liu, S. Srinivasan, M.C. Grady, A.M. Rappe, M. Soroush, Theoretical study of intermolecular chain transfer to polymer reactions of alkyl acrylates, Ind. Eng. Chem. Res. 54 (2015) 4148−4165. Copyright 2015 American Chemical Society.*

A theoretical study of the same CTP reactions for EA (EA2-D1-1(a) shown in Fig. 5.14) revealed that the activation energies and rate constants of the reactions do not change significantly, as the length of the live polymer chain increases. This agrees with previous theoretical studies that the propagation rate constants of MA and MMA are insensitive to the chain length after first propagating step [92]. Such chain-length insensitivity has also been reported for homotermination rate coefficients in free-radical polymerization of acrylates [3]. These findings indicate that it is appropriate to model long live polymer chain with a dimer (trimer) model system, to study CTP reactions.

5.3.2.2 Chain Transfer to D2 and D3 Dead Polymers

Moghadam et al. [50] studied chain transfer to the D2 and D3 dead polymer chains using B3LYP/6−31G(*d,p*) functional. They calculated the bond-dissociation energies of hydrogen atoms of the dead polymer chains (D2 and D3). These hydrogen atoms can be abstracted by a live polymer chain (Fig. 5.15). The calculated bond energies indicated that hydrogen atoms are abstracted most likely via the Y-D2-1 and Y-D3-1 mechanisms, where Y = MA2,

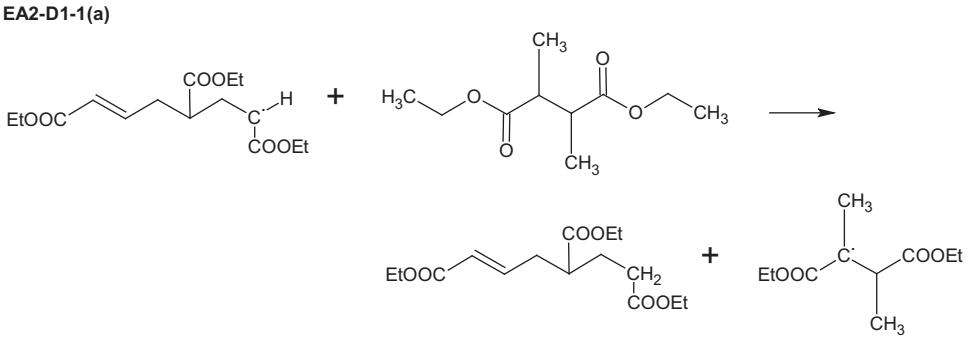

Figure 5.14
Most probable CTP mechanism involving a three EA-unit live chain initiated by $M_2^{\bullet}$. *Reprinted with permission from N. Moghadam, S. Liu, S. Srinivasan, M.C. Grady, A.M. Rappe, M. Soroush, Theoretical study of intermolecular chain transfer to polymer reactions of alkyl acrylates, Ind. Eng. Chem. Res. 54 (2015) 4148–4165. Copyright 2015 American Chemical Society.*

EA2, and *n*-BA-2. Using B3LYP and M06-2X (6−31G(*d,p*), 6−311G(*d*), and 6−311G(*d, p*)) functionals, the most probable mechanisms of chain transfer to D2 and D3 dead polymer chains were found for MA (Fig. 5.16), EA (Fig. 5.17), and *n*BA (Fig. 5.18). These results indicated that the rate coefficient of the MA2-D2-1 mechanism is about three orders of magnitude higher than that calculated for MA2-D1-1, and its energy barrier is lower by about 6 kJ mol^{-1} [50]. Using the M06-2X functional, the same (3 orders of magnitude) difference between the rate coefficients of MA2-D1-1 and MA2-D2-1 was obtained, but a much smaller difference between the energy barriers was calculated.

By applying the B3LYP functional to the EA2-D2-1, EA2-D3-1, *n*-BA2-D2-1, and *n*-BA2-D3-1 mechanisms, and calculating the activation energies and rate coefficients of the most probable chain transfer to D2 and D3 dead polymers of EA and *n*BA, Moghadam et al. [50] found that the activation energies of EA2-D2-1 and *n*-BA2-D2-1 mechanisms are lower than those of EA2-D1-1, EA2-D3-1, *n*-BA2-D1-1 and *n*-BA2-D3-1 mechanisms [50]. These studies revealed that D2 is more likely to undergo CTP reactions than D1 and D3, and that the CTP reactivity of a dead polymer is affected by the type of the carbon atom (tertiary vs. secondary) adjacent to the tertiary carbon atom whose hydrogen is abstracted by a live polymer chain.

5.3.3 Continuum Solvation Models: Integral Equation Formalism-Polarizable Continuum Model and Conductor-Like Screening Model

Moghadam et al. [50] studied solvent (*n*-butanol and *p*-xylene) effects on the kinetics of the most likely CTP mechanisms identified with gas-phase calculations, using two solvation

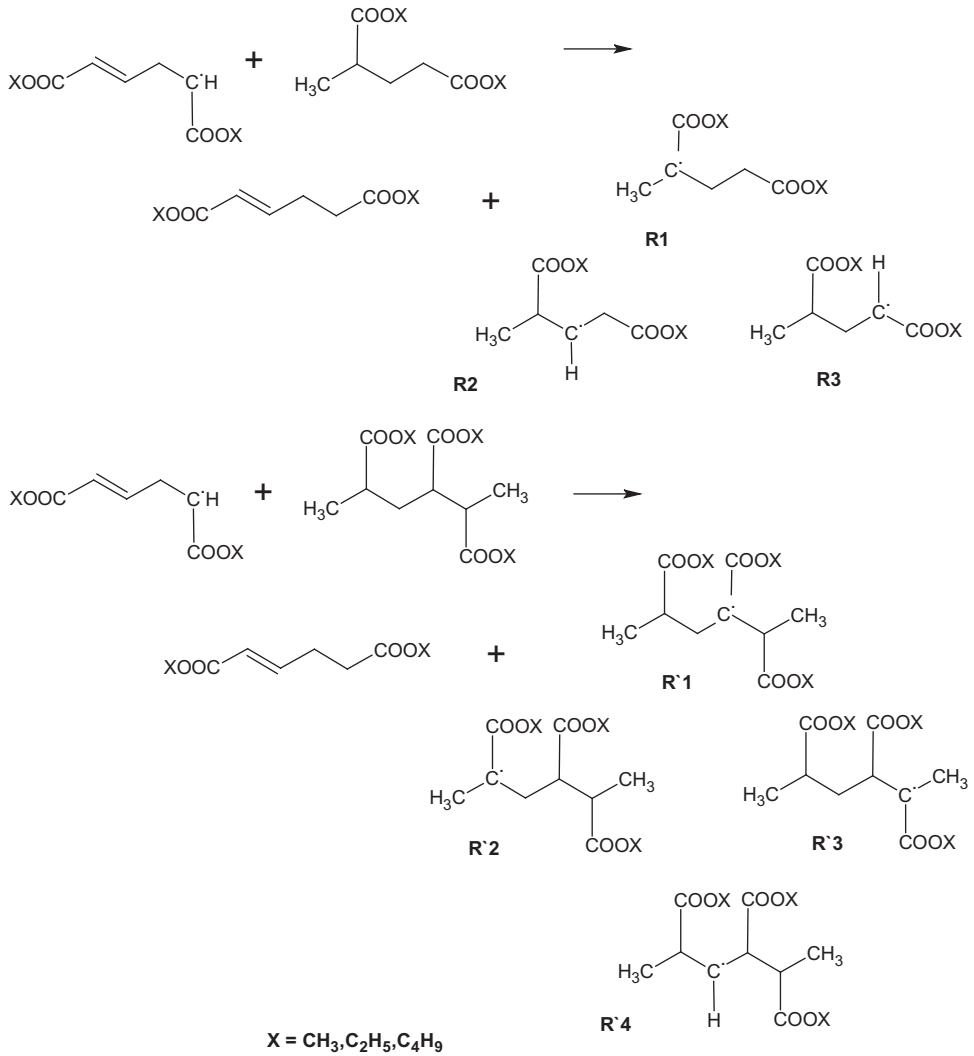

Figure 5.15

Possible chain transfer to the D2 and D3 dead polymers mechanisms for MA, EA, and *n*BA; *Ri* ($i = 1$, 2, and 3) is the radical formed through the Y-D2-*i* mechanism; *R′i* ($i = 1$, 2, 3, and 4) is the radical formed through the Y-D3-*i* mechanism; Y = MA, EA, *n*BA. *Reprinted with permission from N. Moghadam, S. Liu, S. Srinivasan, M.C. Grady, A.M. Rappe, M. Soroush, Theoretical study of intermolecular chain transfer to polymer reactions of alkyl acrylates, Ind. Eng. Chem. Res. 54 (2015) 4148−4165. Copyright 2015 American Chemical Society.*

models, IEF-PCM and COSMO. Activation energies and rate constants of CTP reactions of the alkyl acrylates in *n*-butanol calculated by IEF-PCM, B3LYP and M06-2X functionals, and 6−31G(*d*), 6−31G(*d,p*) and 6−311G(*d,p*) basis sets were found to be very different from the gas-phase values. However, activation energies and rate constants of the same

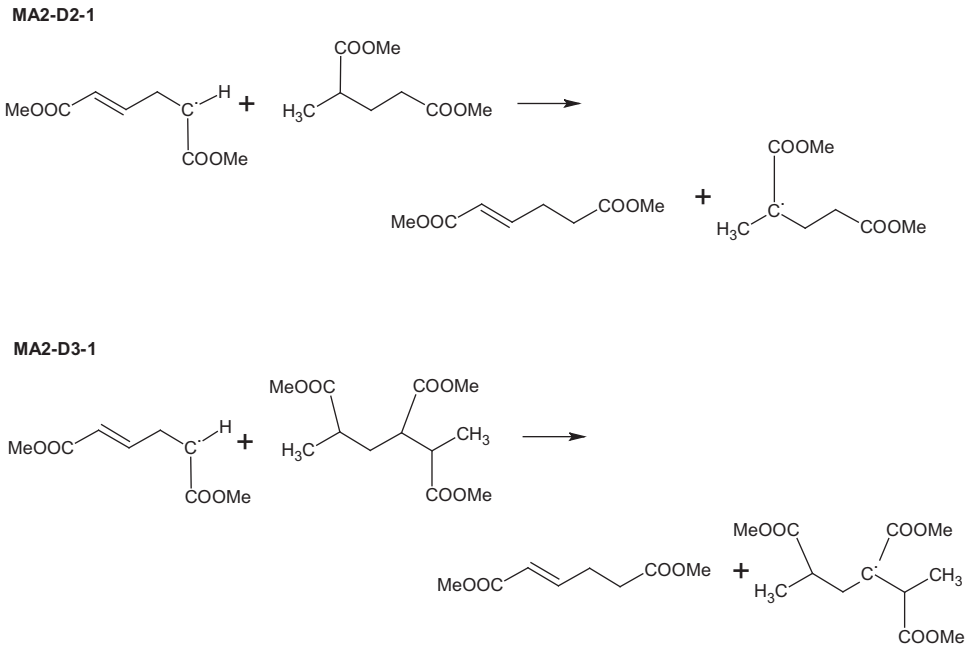

Figure 5.16

Most probable CTP mechanisms involving a two MA-unit live chain initiated by $M_2^{\bullet}$. *Reprinted with permission from N. Moghadam, S. Liu, S. Srinivasan, M.C. Grady, A.M. Rappe, M. Soroush, Theoretical study of intermolecular chain transfer to polymer reactions of alkyl acrylates, Ind. Eng. Chem. Res. 54 (2015) 4148–4165. Copyright 2015 American Chemical Society.*

reactions in *p*-xylene calculated by IEF-PCM and the same functionals and basis sets were very similar to the gas-phase values. These IEF PCM-calculated results point to strong solvent effects of *n*-butanol and weak solvent effects of *p*-xylene. The IEF PCM-calculated activation energies in *n*-butanol are higher than those obtained via gas-phase calculations, resulting in lower rate constants. The effects predicted by IEF-PCM were found not dependent on the end substituent group. The lower rates of the CTP reactions in *n*-butanol agree with the inhibiting effect of *n*-butanol reported by Liang et al. [93]. They found that *n*-butanol inhibits backbiting reactions and consequently reduces the rate of formation of branch points along the polymer backbone during polymerization of *n*BA; *n*-butanol increases the average molecular weights of the polymer.

The application of COSMO, however, did not yield CTP reaction kinetic parameter values very different from gas-phase values for *n*-butanol and *p*-xylene [50]. The insignificant effects of the two solvents on the CTP reactions predicted by COSMO are in agreement with results reported for CTS reactions of acrylates [47] and propagation reactions of acrylonitrile and vinyl chloride [94]. These studies suggested that IEF-PCM is a more appropriate solvation model for studying free-radical polymerization of acrylates than COSMO.

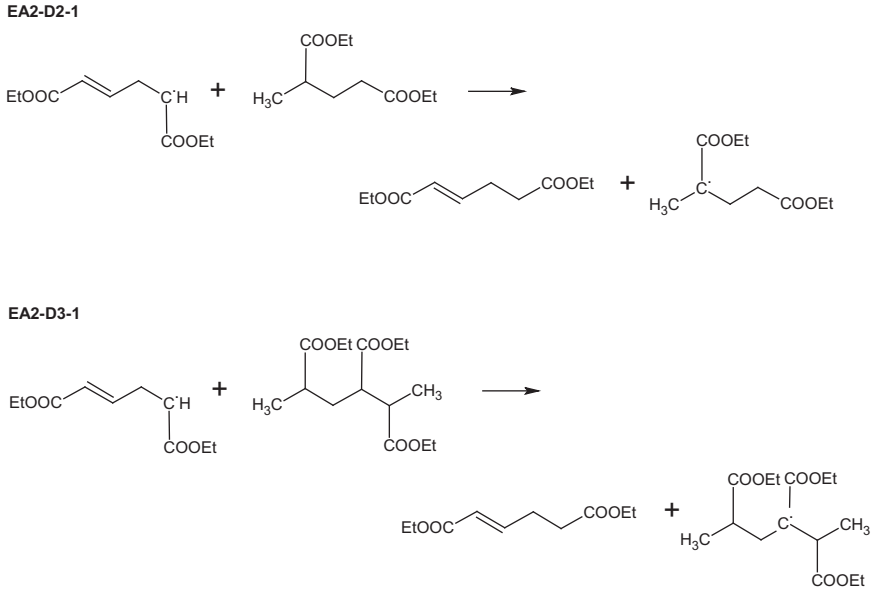

Figure 5.17

Most probable CTP mechanisms involving a two EA-unit live chain initiated by $M_2^{\bullet}$. *Reprinted with permission from N. Moghadam, S. Liu, S. Srinivasan, M.C. Grady, A.M. Rappe, M. Soroush, Theoretical study of intermolecular chain transfer to polymer reactions of alkyl acrylates, Ind. Eng. Chem. Res. 54 (2015) 4148–4165. Copyright 2015 American Chemical Society.*

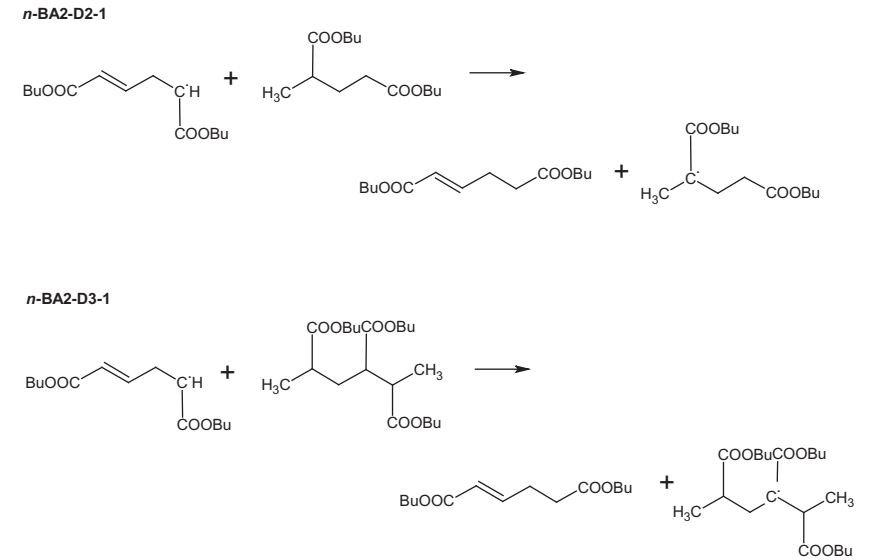

Figure 5.18

Most probable CTP mechanism involving a two *n*BA-unit live chain initiated by $M_2^{\bullet}$. *Reprinted with permission from N. Moghadam, S. Liu, S. Srinivasan, M.C. Grady, A.M. Rappe, M. Soroush, Theoretical study of intermolecular chain transfer to polymer reactions of alkyl acrylates, Ind. Eng. Chem. Res. 54 (2015) 4148–4165. Copyright 2015 American Chemical Society.*

5.3.4 Intermolecular CTP Summary

Thermodynamic and kinetic parameters (activation energies, enthalpies of reaction, Gibbs free energies, frequency factors, and rate constants) of intermolecular CTP reactions can be calculated reliably using computational quantum chemistry. The abstraction of a tertiary hydrogen from a dead polymer chain is the most favorable intermolecular CTP mechanism in alkyl acrylates. The length of a live polymer chain and the end substituent group of the monomer forming a live polymer chain were found to have little effects on the energy barriers and transition-state geometries in all CTP mechanisms that were explored [50]. IEF-PCM predicted CTP energy barriers larger than those calculated in the gas phase, but the application of COSMO led to CTP energy barriers similar to those calculated in the gas phase. IEF-PCM predicted larger CTP energy barriers in *n*-butanol than in *p*-xylene.

5.4 Chain Transfer to Solvent Reactions

The production of resins with low solvent contents and low molecular weights has been achieved via high temperature ($>100^{\circ}C$) solution free-radical polymerization [1,10,95]. It has been reported [2,13–15] that at high temperatures, propagating free radicals undergo secondary reactions such as β-scission and CTM, polymer and solvent reactions. A better understanding of solvent effects in high-temperature free-radical polymerization can lead to improved process efficiency and quality of acrylic resins.

5.4.1 Prior Experimental Knowledge

Polymerization reactions, such as β-scission, CTS, and radical transfer to solvent from initiator radical, in high-temperature polymerization of *n*BA were observed using liquid chromatography-electrospray ionization-tandem mass spectrometry [96]. In thermal polymerization of EA, MA, and ethyl methacrylate (EMA), CTS rate coefficients for various solvents, such as hydrocarbons, alcohols, ketones, acids, and esters, were estimated from polymer sample measurements [97,98]. Moreover, the effect of solvent in the homopolymerization of *n*BA was investigated [99]. It was reported that, as the solvent concentration increases, the rate of CTS reactions and the rate of formation of shorter chains increases, and these shorter chains terminate faster than longer ones [99].

Polymer chains with end groups formed by chain transfer reactions were identified using ESI-FTMS [14] and MALDI [100] in self-initiated polymerization of MA, EA, and *n*BA ($100-180^{\circ}C$). The presence of these end groups was further confirmed using NMR analyses of the polymers [14]. Chain transfer and radical propagation rate coefficients of acrylates [33,34,101] were determined using pulsed-laser polymerization/size exclusion chromatography at various temperatures below $30^{\circ}C$ [36,37,102]. In the absence of chain transfer agents, self-regulation and polymers with uniform chain lengths were observed in

thermal polymerization of alkyl acrylates [103]. These observations were attributed to the self-regulatory capability of CTS, polymer, and monomer mechanisms. Although the existence of CTS reactions was known for many decades [30,31], before the study of these reactions using computational quantum chemistry [47,49], little was known about exact mechanisms of CTS reactions.

5.4.2 Knowledge Gained Using Quantum Chemical Calculations

While experimental studies provided a useful overall understanding of chain transfer reactions, they were not able to conclusively identify the involved individual reaction mechanisms and reacting species. However, quantum chemical calculations have been able to identify the most likely reaction mechanisms and reacting species.

The stability of transition state geometries can be increased in the presence of a solvent [100]. Different solvent continuum models have been proposed and used to study solvent effects on solutes [104,105]. In continuum models, a solvent is treated as a dielectric continuum mean field polarized by the solute in the continuum. While the self-consistent reaction field method places the solute in a spherical cavity [106], the polarizable continuum model (PCM) introduces molecular shape for the cavity [107,108]. However, these models cannot describe the microscopic structure of the solvent-solute interactions. PCM was applied to predict the propagation rate coefficient of acrylic acid in the presence of toluene [105]. Conductor-like screening model [109] is another approach for polarized continuum calculations in which the surrounding medium (solvent) is assumed to be a conductor rather than a dielectric, simplifying the electrostatic interactions between the solvent and solute. The effect of solvents with different dielectric constants on the propagation rate coefficients in free-radical polymerization of acrylonitrile and vinyl chloride was investigated [94]. COSMO was also applied to predict nonequilibrium solvation energies of biphenyl-cyclohexane-naphthalene [110]. The conductor-like screening model for real solvents (COSMO-RS) is another solvation model. Deglmann et al. [111,112] used COSMOS-R to estimate rate coefficients of propagation reactions in free-radical solution polymerization of acrylates.

The rest of this section presents a computational and theoretical study of CTS reactions of MA, EA, and *n*BA homopolymerizations in butanol (polar, protic), methyl ethyl ketone (MEK) (polar, aprotic), and *p*-xylene (nonpolar) [47]. Moghadam et al. [47] investigated the abstraction of a hydrogen from *n*-butanol, MEK, and *p*-xylene by a live polymer chain to identify the most likely mechanisms of CTS reactions in MA, EA, and *n*BA homopolymerizations. They also studied the effect of the type of the self-initiating monoradical that initiated the live chain participating in the CTS reactions. They used the B3LYP, X3LYP, M06-2X functionals and with the 6−31G (*d,p*), 6−311G(*d,p*), and 6−311G(*d,p*) basis sets to optimize the molecular geometries of reactants, products, and

transition states in the gas phase. Optimized reactants and transition states were confirmed by Hessian calculations. They used the RRHO approximation to calculate energy barriers relative to the energy of reactants. They calculated activation energies and rate constants of CTS reactions using transition-state theory. Scaling factors of 0.961, 0.966, and 0.967 [113] were used for the B3LYP functional with the 6−31G(*d,p*), 6−311G(*d*), and 6−311G(*d,p*) basis sets, respectively, to calculate activation entropies, temperature corrections, and zero point vibrational energies. They considered quantum tunneling in the reactions involving the transfer of an hydrogen atom [114,115]. They performed all calculations using GAMESS [84]. They applied PCM and COSMO solvation models to study the chain transfer reactions. Because of the high computational cost of simulating chain transfer from long live chains to a solvent, live polymer chains with only two monomer units were considered in these CTS studies.

5.4.2.1 Most likely chain transfer to solvent mechanisms for MA, EA, and nBA

Moghadam et al. [47] considered the CTS reaction mechanisms shown in Fig. 5.19 for *n*-butanol, MEK, and *p*-xylene. In these reactions, a hydrogen atom is abstracted by a live polymer chain from a solvent molecule. Moghadam et al. [47] calculated bond dissociation energy defined as the energy difference between a solvent molecule and bond-cleavage products (a hydrogen radical and a solvent radical) [116]:

$$\text{Bond Dissociation Energy} = E_{(\text{Bond-Cleavage Products})} - E_{(\text{Solvent})} \tag{5.1}$$

The calculated bond dissociation energies suggested that the C−H breaking bonds in the CTB1-2, CTM1-2, and CTX1-2 mechanisms are weaker than those in other mechanisms. A radical formed by the cleavage of a methylene group C−H bond is more stable than that formed by the cleavage of a methyl group C−H bond. This suggests that hydrogen abstraction from a methylene group is favored over that from a methyl group in *n*-butanol. Mulliken charge analysis also showed that the methylene carbon atom (0.047) next to the oxygen atom is much more positive than the oxygen atom (−0.573), making the methylene carbon more likely to release an hydrogen atom. Calculated thermodynamic and kinetic parameters (activation energies, Gibbs free energies, frequency factors, enthalpies of reaction, and rate constants) of the most likely mechanisms of CTS reactions of MA, EA, and *n*BA indicated that the activation energy of chain transfer to *n*-butanol is lower than those of MEK and *p*-xylene reactions, and the rate constant for chain transfer to *n*-butanol is higher than those of MEK and *p*-xylene [47]. The polar and protic nature of *n*-butanol facilitates the transfer of a hydrogen atom to a polymer chain. *p*-Xylene and MEK lack a labile hydrogen atom to transfer.

Moghadam et al. [47] reported that activation energies and rate constants calculated by M06-2X, a hybrid meta-GGA functional, were higher than those calculated by B3LYP and X3LYP. Their findings for the CTS reactions agreed with their earlier findings for CTM

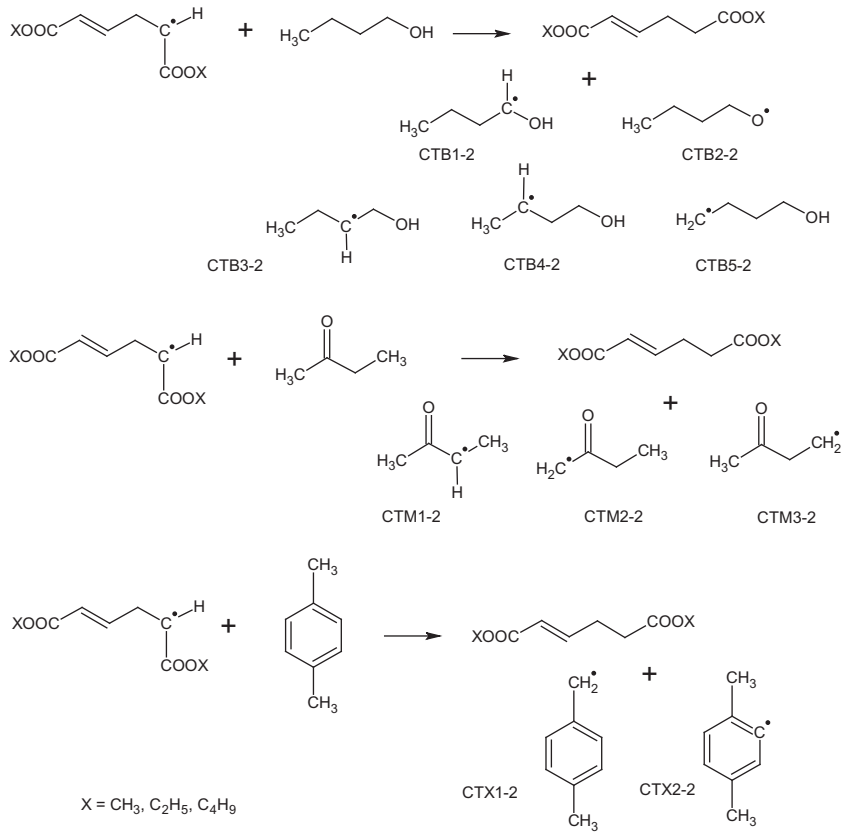

Figure 5.19

End-chain transfer to solvent (CTS) reactions involving a two-monomer unit live chain initiated by $M_2^{\bullet}$ shown in Fig. 5.1. *CTB*, chain transfer to *n*-butanol; *CTM*, chain transfer to methyl ethyl ketone; *CTX*, chain transfer to *p*-xylene. *Reprinted with permission from N. Moghadam, S. Srinivasan, M. C. Grady, A.M. Rappe, M. Soroush, Theoretical study of chain transfer to solvent reactions of alkyl acrylates, J. Phys. Chem. A 118 (2014) 5474−5487. Copyright 2014 American Chemical Society.*

reactions of alkyl acrylates [51]. Their calculated kinetic parameters for chain transfer to *n*-butanol, MEK, and *p*-xylene for EA were similar to their calculated kinetic parameters for the same reactions for *n*BA, indicating that the length of the end-substituent group of a live polymer chain has a negligible effect on the kinetics of the reactions [47]. The activation energy of chain transfer to *p*-xylene for *n*BA that they calculated using M06−2X/6−31G(*d,p*) functional agrees with that estimated from laboratory measurements [13]. However, their theoretically predicted rate constant is four orders of magnitude smaller than the experimentally estimated one. They attributed this difference to underestimation of the solvent-based entropic effects and frequency factor. These results point to a higher capability of hybrid meta-GGA functionals such as M06−2X to account for van der Waals

interactions [81,83], permitting these functionals to predict barrier heights more accurately than those predicted by B3LYP. Hybrid meta-GGA functionals, however, do not accurately account for all solvent interactions. An alternative approach is to pair other DFT functionals with van der Waals corrections, such as the TS, D2, or D3 [117–119] methods.

5.4.2.2 Chain transfer to n-butanol, sec-butanol, and tert-butanol

Moghadam et al. [47] studied the theoretical mechanisms of chain transfer to *n*-butanol, *sec*-butanol, and *tert*-butanol shown in Fig. 5.20. A live polymer chain can abstract an hydrogen atom from different atoms of solvents. Moghadam et al. [47] calculated bond-dissociation energies of all available hydrogen atoms in the three solvents and reported that the weakest C–H bond is the one that is broken in the CTBsec1–2 mechanism. This agrees with their earlier finding that a methylene carbon atom is more capable of releasing an hydrogen atom than a methyl carbon and an oxygen atom [47]. The methylene carbon atom next to the oxygen in *sec*-butanol, which has a Mulliken charge of 0.152, is more likely to release an hydrogen than the other methylene carbon atom, which has a Mulliken charge of −0.228 [47]. As bond-dissociation energies calculated for CTBtert1–1 and CTBtert1–2 mechanisms are similar, these mechanisms are equally likely to occur in chain transfer to *tert*-butanol. The computational study showed that among *n*-butanol, *sec*-butanol, and *tert*-butanol, *tert*-butanol has the lowest and *sec*-butanol has the highest chain transfer rate

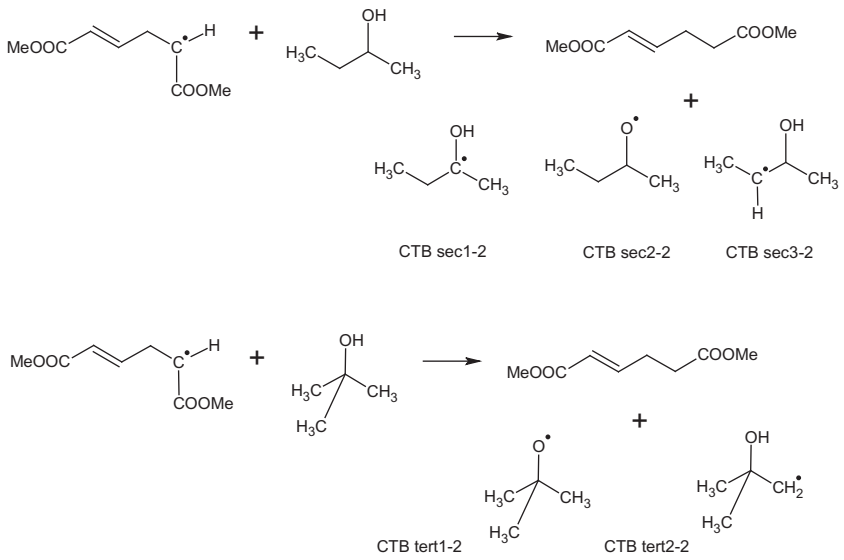

Figure 5.20

End-chain transfer to *sec*-butanol and *tert*-butanol reactions for MA involving a two-monomer unit live chain initiated by $M_2^{\bullet}$ shown in Fig. 5.1. *Reprinted with permission from N. Moghadam, S. Srinivasan, M.C. Grady, A.M. Rappe, M. Soroush, Theoretical study of chain transfer to solvent reactions of alkyl acrylates. J. Phys. Chem. A 118 (2014) 5474–5487. Copyright 2014 American Chemical Society.*

coefficient [47]. These findings are in agreement with the experimentally estimated chain transfer to *n*-butanol, *sec*-butanol and *tert*-butanol rate coefficients in MA polymerization at 80°C [97]. A comparison of experimentally estimated [97,120] and theoretically predicted values [47] of chain transfer to *n*-butanol, *sec*-butanol and *tert*-butanol rate coefficients in MA polymerization at 80°C, given in Table 5.1, indicates that: (1) the M06-2X-predicted values are closer to the experimentally estimated ones; (2) the M06-2X-predicted values of chain transfer to *n*-butanol and *sec*-butanol rate coefficients are very close to the experimentally estimated ones, and (3) the chain transfer to *tert*-butanol rate coefficients predicted by M06-2X and B3LYP are, respectively, approximately four and six orders of magnitude smaller than the experimentally estimated one [47].

5.4.2.3 Predictions with continuum solvation models PCM and COSMO

Moghadam et al. [47] also predicted kinetic parameters of the most likely CTS reaction mechanisms (CTB1-2, CTM1-2, and CTX1-2) using PCM and COSMO solvation models. As Table 5.2 indicates, while the activation energy and rate coefficient of chain transfer to *n*-butanol calculated with PCM were significantly different from their gas-phase values, those of chain transfer to MEK and *p*-xylene were similar to their gas-phase values. The PCM-calculated activation energy for *n*-butanol was found to be higher than those obtained via gas-phase calculations; the PCM-calculated rate constant for *n*-butanol was lower.

Table 5.1: Activation Energy (E_a), Enthalpy of Activation ($\Delta H^{\ddagger}$), and Gibbs Free Energy of Activation ($\Delta G^{\ddagger}$) in kJ mol^{-1}; Tunneling Factor (k_w for Wigner Correction); and Frequency Factor (A) and Rate Constant (k: Without Tunneling and kw: With Tunneling) in M^{-1} s^{-1}, for CTB1-2, CTBsec1-2, and CTBtert1-2 Mechanisms of MA at 298 K [47]

		n-Butanol	*sec*-Butanol	*tert*-Butanol
B3LYP/6-31G(*d*,*p*)	E_a	45.50	45.30	79.50
	$\Delta H^{\ddagger}$	40.60	40.30	74.00
	$\Delta G^{\ddagger}$	95.10	93.90	127.00
	$\log_e A$	12.65	13.02	13.26
	k	3.30E-03	5.20E-03	6.63E-09
	k_w	3.27	3.25	3.15
	k_w	1.07E-02	1.69E-02	2.10E-08
M06-2X/6-31G(*d*,*p*)	E_a	22.90	24.10	64.30
	$\Delta H^{\ddagger}$	17.90	19.20	59.40
	$\Delta G^{\ddagger}$	78.40	77.20	109.70
	$\log_e A$	10.25	11.27	14.34
	k	2.78E + 00	4.60E + 00	9.00E-06
	k_w	3.41	3.37	3.28
	k_w	9.48E + 00	1.55E + 01	2.95E-05
Experimental [97,120]	k (353 K)	1.10E + 01	5.50E + 01	1.50E + 00
B3LYP/6-31G(*d*,*p*)	k (353 K)	5.76E-02	8.93E-02	9.87E-07
M06-2X/6-31G(*d*,*p*)	k (353 K)	1.16E + 01	2.10E + 01	5.20E-04

Table 5.2: Activation Energy (E_a), Enthalpy of Activation ($\Delta H^{\ddagger}$), and Gibbs Free Energy of Activation ($\Delta G^{\ddagger}$) in kJ mol^{-1}; Frequency Factor (A) and Rate Constant (k) in M^{-1} s^{-1}, for CTB1-2, CTM1-2, and CTX1-2 Mechanisms of MA, EA, and *n*BA at 298 K, Using PCM and COSMO [47]

	M06-2X/6−31G(*d,p*)		M06-2X/6−31G(*d,p*)		M06−2X/6−31G(*d,p*)	
	COSMO	PCM	COSMO	PCM	COSMO	PCM
MA	CTB1-2		CTM1-2		CTX1-2	
E_a	23.50	38.10	51.00	48.40	51.60	56.50
$\Delta H^{\ddagger}$	18.40	33.20	46.20	43.40	46.60	51.50
$\Delta G^{\ddagger}$	78.50	84.70	96.60	103.50	96.30	105.60
$\log_e A$	10.49	13.86	14.22	10.60	14.82	13.02
K	2.73E + 00	2.20E-01	1.72E-03	1.31E-04	2.46E-03	5.63E-05
EA	CTB1-2		CTM1-2		CTX1-2	
E_a	20.30	34.40	47.10	46.30	51.30	59.50
$\Delta H^{\ddagger}$	15.30	28.60	42.20	40.70	46.50	54.20
$\Delta G^{\ddagger}$	73.50	80.20	97.10	98.40	94.10	105.60
$\log_e A$	11.09	14.21	12.41	11.57	15.42	13.62
K	1.81E + 01	1.38E + 00	1.36E-03	8.11E-04	5.10E-03	3.10E-05
BA	CTB1-2		CTM1-2		CTX1-2	
E_a	18.00	35.50	39.10	45.40	54.20	57.20
$\Delta H^{\ddagger}$	13.50	30.40	34.20	40.40	49.10	51.60
$\Delta G^{\ddagger}$	75.30	82.60	88.40	98.30	98.50	106.00
$\log_e A$	9.53	13.26	13.01	11.21	14.82	13.01
K	9.63E + 00	3.43E-01	6.26E-02	8.13E-04	8.62E-04	4.20E-05

As *p*-xylene is nonpolar, the application of PCM did not alter the stability of reactants or the transition states considerably. However, as *n*-butanol and MEK are both polar, the stability of the reactants and transition states were affected strongly by PCM. Because MEK is more polar than *n*-butanol, PCM stabilizes the transition state of CTM1-2 more than that of CTB1-2. For MEK, the change in the stability of CTM1-2 transition state was similar to that of the reactants. Moghadam et al. [47] also conducted PCM calculations to study CTB1-2, CTM1-2, and CTX1-2 mechanisms for EA and *n*BA. They found that PCM has a strong effect on the calculated activation energies and rate constants of the chain transfer to *n*-butanol reactions, but very weak effects on those of chain transfer to MEK and *p*-xylene. As Table 5.2 indicates, for the three monomers that have different end substituent groups, PCM's effects on their predicted kinetic parameter values were similar. Liang et al. [93] studied polymerization of *n*BA in *n*-butanol and reported that *n*-butanol inhibits backbiting reactions.

As Table 5.2 indicates, unlike PCM, COSMO does not alter the relative stability of the reactants and the transition states noticeably, implying that COSMO is unable to describe effects of the

solvents on the CTS reactions. In COSMO, nonelectrostatic solute-solvent interactions, such as dispersion, repulsion, and electrostatic interactions, are accounted for. However, because COSMO uses a simple model to describe nonelectrostatic interactions, its predictions are very inaccurate when the involved molecules have interactions, such as hydrogen bonding. The small effect of the inclusion of COSMO on the predicted kinetic parameters of the CTS reactions is in agreement with findings reported by other investigators [94].

5.4.2.4 Effect of the type of initiating radical

Fig. 5.21 shows the most likely CTS reaction mechanisms of a two-monomer unit live polymer chain initiated by $M_1^{\bullet}$, and Table 5.3 presents the kinetic parameter values of the CTB1-1, CTM1-1 and CTX1-1 reactions calculated in the gas phase [47]. These calculated rate coefficients are comparable to those of a two-monomer unit live polymer chain initiated by $M_2^{\bullet}$; the type of the initiating radicals has an insignificant effect on the rates of the CTS reactions.

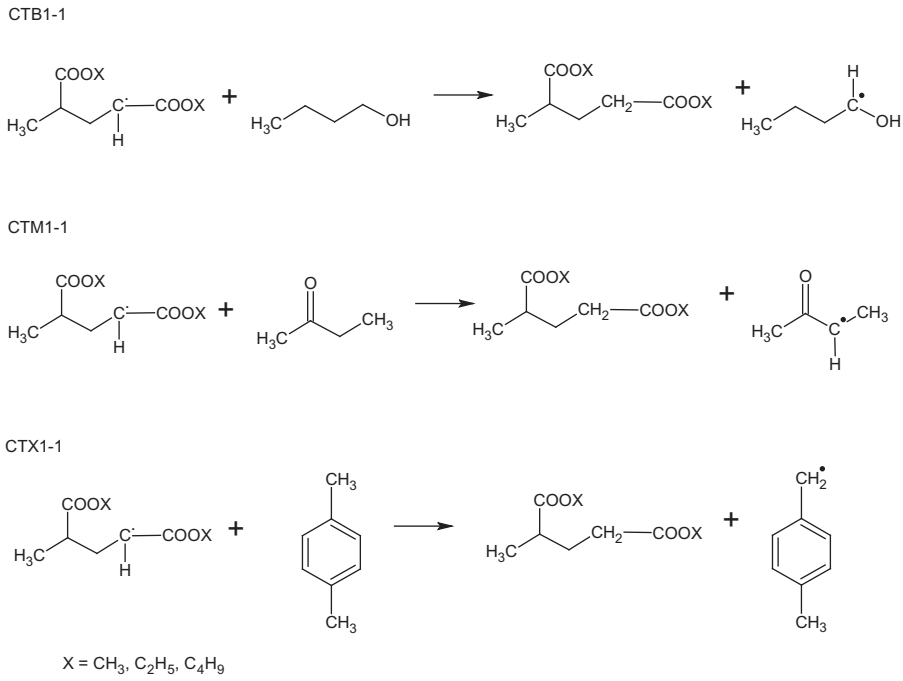

Figure 5.21

Mechanisms for CTS reactions involving a two-monomer unit live chain initiated by $M_1^{\bullet}$ shown in Fig. 5.1. *Reprinted with permission from N. Moghadam, S. Srinivasan, M.C. Grady, A.M. Rappe, M. Soroush, Theoretical study of chain transfer to solvent reactions of alkyl acrylates. J. Phys. Chem. A 118 (2014), 5474–5487. Copyright 2014 American Chemical Society.*

Table 5.3: Activation Energy (E_a), Enthalpy of Activation ($\Delta H^{\ddagger}$), and Gibbs Free Energy of Activation ($\Delta G^{\ddagger}$) in kJ mol^{-1}; Tunneling Factor (k_w for Wigner Correction); and Frequency Factor (A) and Rate Constant (k: Without Tunneling and k_w: with Tunneling) in M^{-1} s^{-1}, for CTB1-1, CTM1-1, and CTX1-1 Mechanisms of MA, EA, and *n*BA at 298 K [47]

	B3LYP/ 6−31G(*d,p*)	M06-2X/ 6−31G(*d,p*)	B3LYP/ 6−31G(*d,p*)	M06-2X/ 6−31G(*d,p*)	B3LYP/ 6−31G(*d,p*)	M06-2X/ 6−31G(*d, p*)
MA	**CTB1-1**		**CTM1-1**		**CTX1-1**	
E_a	48.40	23.00	67.40	52.20	66.40	56.10
$\Delta H^{\ddagger}$	42.60	18.30	61.60	47.40	61.20	51.30
$\Delta G^{\ddagger}$	93.70	75.80	111.30	102.10	110.50	107.50
$\log_e A$	14.21	11.45	14.82	12.41	14.82	12.05
K	4.87E-03	8.73E + 00	4.92E-06	1.70E-04	6.27E-06	2.51E-05
k_w	3.27	3.41	3.62	3.19	3.59	3.33
k_w	1.59E-02	2.97E + 01	1.78E-05	5.42E-04	2.25E-05	8.35E-05
EA	**CTB1-1**		**CTM1-1**		**CTX1-1**	
E_a	46.30	22.30	69.50	48.10	67.00	53.40
$\Delta H^{\ddagger}$	41.20	17.20	63.60	43.50	62.10	48.40
$\Delta G^{\ddagger}$	97.00	75.40	107.70	94.30	105.50	102.00
$\log_e A$	12.05	10.85	15.42	12.05	16.02	14.22
K	1.30E-03	6.36E + 00	4.18E-06	6.30E-04	1.63E-05	6.50E-04
k_w	3.28	3.50	3.63	3.17	3.56	3.30
k_w	4.26E-03	2.22E + 01	1.52E-05	1.99E-03	5.80E-05	2.15E-03
BA	**CTB1-1**		**CTM1-1**		**CTX1-1**	
E_a	45.60	21.20	65.50	43.10	64.20	56.10
$\Delta H^{\ddagger}$	41.10	16.50	60.40	38.50	59.10	51.50
$\Delta G^{\ddagger}$	95.70	74.30	106.30	94.50	107.20	103.00
$\log_e A$	12.41	11.21	16.02	12.17	15.42	13.62
K	2.50E-03	1.42E + 01	2.99E-05	5.40E-03	2.77E-05	1.20E-04
k_w	3.31	3.48	3.57	3.16	3.61	3.36
k_w	8.27E-03	4.94E + 01	1.07E-04	1.70E-02	1.00E-04	4.03E-04

To study the influence of the type of the initiating radicals on the CTS reactions in solution, Moghadam et al. [47] applied PCM to the reactions. The calculated activation energies and rate constants of the CTB1-1, CTM1-1, and CTX1-1 reactions are listed in Table 5.4. The activation energies and rate coefficients of the CTS reactions of the live chains initiated by $M_1^{\bullet}$ are different, respectively, by ± 3 kJ mol^{-1} and one order of magnitude from those of the live chains initiated by $M_2^{\bullet}$ (Table 5.2) [47]. The ~ 16 kJ mol^{-1} increase in the activation energies and the two orders of magnitude decreases in the rate coefficients calculated using PCM relative to those calculated in the gas phase (reported in Table 5.3) show the significant effect of PCM on the kinetic parameters of the CTB1-1 mechanism. However, COSMO (Table 5.4) predicted similar rate coefficients for CTS reactions of live chains initiated by the

Table 5.4: Activation Energy (E_a), Enthalpy of Activation ($\Delta H^{\ddagger}$), and Gibbs Free Energy of Activation ($\Delta G^{\ddagger}$) in kJ mol^{-1}; Frequency Factor (A) and Rate Constant (k) in M^{-1} s^{-1}, for CTB1-1, CTM1-1, and CTX1-1 Mechanisms of MA, EA, and *n*BA at 298 K, Using PCM and COSMO [47]

	M06-2X/6-31G(*d,p*)		M06-2X/6-31G(*d,p*)		M06-2X/6-31G(*d,p*)	
	COSMO	PCM	COSMO	PCM	COSMO	PCM
MA	**CTB1-1**		**CTM1-1**		**CTX1-1**	
E_a	24.50	39.30	50.50	50.10	53.20	57.50
$\Delta H^{\ddagger}$	19.10	33.90	45.30	45.40	48.30	51.60
$\Delta G^{\ddagger}$	79.50	86.10	97.20	102.00	102.40	104.800
$\log_e A$	10.49	13.62	13.50	11.57	12.78	13.26
K	1.82E + 00	1.10E-01	1.00E-03	1.80E-04	1.70E-04	4.75E-05
EA	**CTB1-1**		**CTM1-1**		**CTX1-1**	
E_a	23.40	35.50	48.20	48.60	50.30	58.40
$\Delta H^{\ddagger}$	17.60	30.30	42.60	44.00	44.60	53.40
$\Delta G^{\ddagger}$	77.50	80.80	97.30	102.70	93.50	108.70
$\log_e A$	10.73	13.98	13.02	10.85	15.30	12.05
K	3.60E + 00	7.10E-01	1.60E-03	1.60E-04	6.70E-03	9.90E-06
***n*BA**	**CTB1-1**		**CTM1-1**		**CTX1-1**	
E_a	23.50	37.20	45.40	48.10	58.10	57.00
$\Delta H^{\ddagger}$	18.20	31.70	40.30	43.40	53.40	52.50
$\Delta G^{\ddagger}$	78.60	82.00	91.80	100.10	102.20	104.00
$\log_e A$	10.13	14.46	13.62	11.69	14.94	13.50
K	1.90E + 00	5.70E-01	9.00E-03	4.40E-04	2.00E-04	7.44E-05

$M_2^{\bullet}$ and $M_1^{\bullet}$ radicals; the activation energies were at most 6 kJ mol^{-1} larger (rate coefficients one order of magnitude smaller) than those obtained for the CTB1-2, CTM1-2, and CTX1-2 mechanisms involving live chains initiated by $M_2^{\bullet}$ (Table 5.2). The COSMO-predicted kinetic parameter values were similar to the gas phase values (Table 5.3).

5.4.2.5 *Effects of live polymer chain length*

To study the effects of live polymer chain-length on CTS reactions, Moghadam et al. [47] considered the CTB1-2′, CTM1-2′, and CTX1-2′ mechanisms involving three-monomer unit live chains of MA, EA, and *n*BA initiated by $M_2^{\bullet}$ (Fig. 5.22). They found that the kinetic parameters of the CTS reactions do not appreciably depend on the live polymer chain length. The geometries of the transition states of the CTB1-2′, CTM1-2′ and CTX1-2′ mechanisms were found to be quite similar to those of the CTB1-2, CTM1-2 and CTX1-2 mechanisms in which two-monomer unit live chains initiated by $M_2^{\bullet}$ were involved [47], implying that the length of live polymer chains does not affect the geometry of the reaction transition states. These findings are in agreement with results from CTM studies [51] and propagation reactions of alkyl acrylates [92]. Moghadam et al. [47] also conducted these

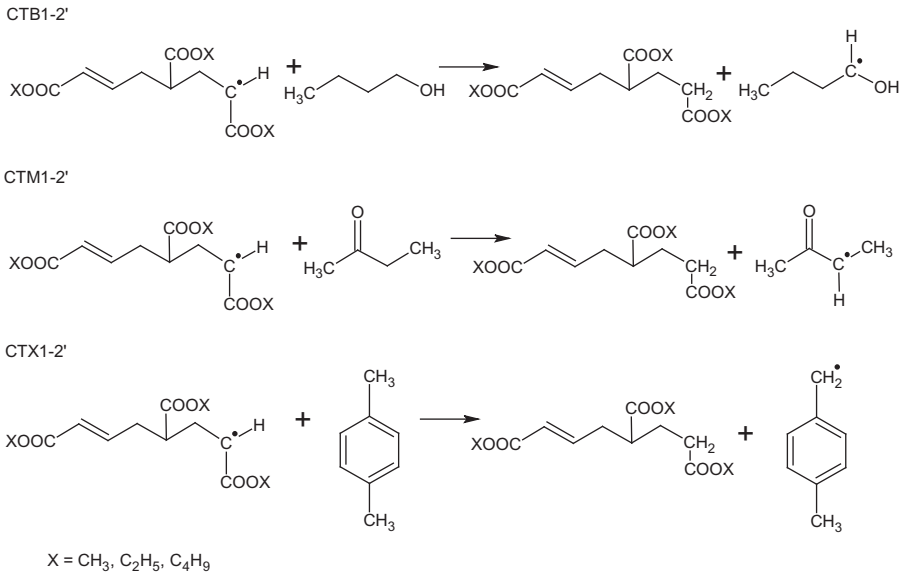

Figure 5.22

Mechanisms for CTS reactions involving a three-monomer unit live chain initiated by $M_2^{\bullet}$ shown in Fig. 5.1. *Reprinted with permission from N. Moghadam, S. Srinivasan, M.C. Grady, A.M. Rappe, M. Soroush, Theoretical study of chain transfer to solvent reactions of alkyl acrylates, J. Phys. Chem. A 118 (2014) 5474–5487. Copyright 2014 American Chemical Society.*

same studies in the solution phase using PCM; the PCM-predicted results were not different from the gas-phase results.

5.4.3 CTS Summary

This section reviewed recent advances made in better understanding mechanisms of chain transfer to *n*-butanol, MEK, and *p*-xylene in polymerization of three alkyl acrylates, using first-principles quantum-chemical calculations [47]. The theoretical studies revealed that for MA, EA, and *n*BA homopolymerization in butanol, MEK, and *p*-xylene, the following CTS mechanisms are most likely: the abstraction of a hydrogen from the methylene group next to the oxygen atom of an *n*-butanol molecule by a live polymer chain, the abstraction of a hydrogen from the methylene group of an MEK molecule, and the abstraction of a hydrogen from a methyl group in a *p*-xylene molecule. Among *n*-butanol, *tert*-butanol and *sec*-butanol, *tert*-butanol has the highest CTS energy barrier and the lowest rate coefficient. Chain transfer to *sec*-butanol and *n*-butanol reactions have comparable kinetic parameter values. The activation energy of the most likely mechanism of chain transfer from a two-monomer unit live *n*BA polymer chain initiated by $M_2^{\bullet}$ to *p*-xylene calculated using M06-2X/6-31G(*d,p*) was found to be comparable to those estimated from polymer sample

measurements. The kinetic parameter values of the chain transfer to *n*-butanol reactions calculated using PCM were found to be very different from the values calculated in the gas phase. However, the application of PCM did not appreciably affect the stability of the reactants and the transition states in chain transfer to MEK and *p*-xylene. COSMO did not predict a solvent effect on the kinetics of the CTS reactions of MA, EA, and *n*BA. The activation energies and rate constants of the CTS reactions were found to be nearly independent of the length of the live polymer chains and the type of the self-initiated monoradicals that initiated the live polymer chains.

5.5 Backbiting and β-Scission Reactions

The occurrence of intermolecular and intramolecular CTP reactions in thermal polymerization of alkyl acrylates and methacrylates has been studied extensively [121–125]. In an intramolecular chain transfer reaction (backbiting), a live polymer chain abstracts a hydrogen from a tertiary carbon on its backbone and forms a midchain radical (MCR) (Fig. 5.23). The MCR, a tertiary radical, can then undergo propagation, β-scission, or termination.

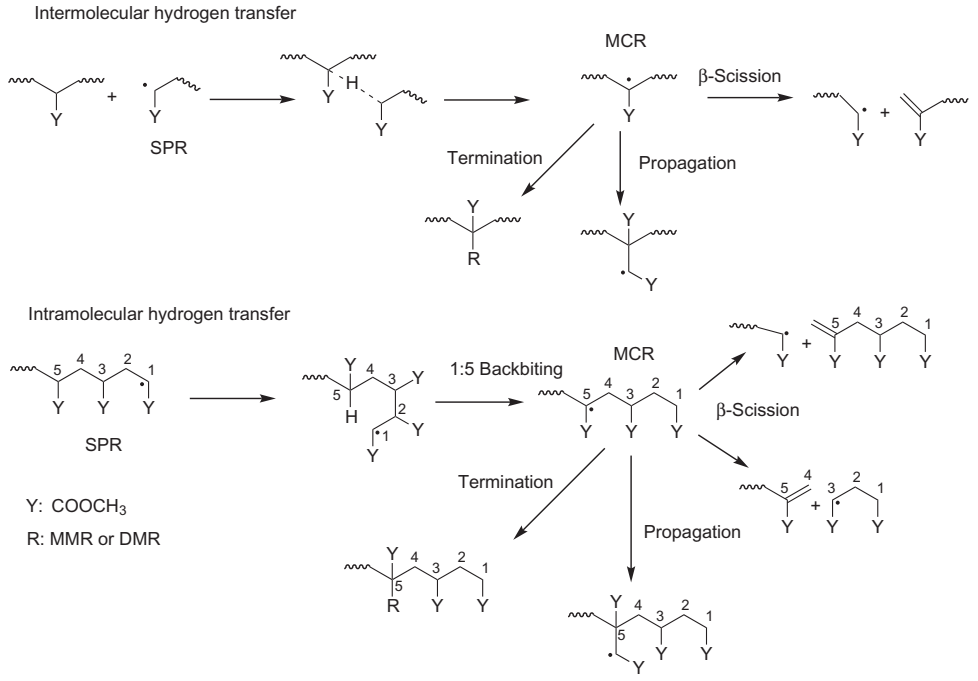

Figure 5.23

Intermolecular and intramolecular hydrogen transfer reactions in high-temperature spontaneous homopolymerization of alkyl acrylates. *Reprinted with permission from S. Liu, S. Srinivasan, M.C. Grady, M. Soroush, A.M. Rappe, Backbiting and beta-scission reactions in free- radical polymerization of methyl acrylate, Int. J. Quantum Chem. 114 (2014) 345–360. Copyright 2014 American Chemical Society.*

5.5.1 Prior Experimental Knowledge

It was reported that in intramolecular hydrogen transfer, a six-membered ring transition state is favored [121]. However, no direct evidence of the existence of cyclic (6- or 8- or 10-membered ring) transition states in radical polymerization of acrylates was available. It was known that polymer-chain branching occurs when a MCR participates in a propagation reaction [124,125]; at high ($>50\%$) monomer concentrations, intermolecular chain transfer, and long chain branching are more likely [124]; at low monomer concentrations, intramolecular chain transfer (backbiting) [125] and short-chain branching [70,75,123] are more probable. Studies using ^{13}C-NMR spectroscopy [14,38,60,63,70,75,123,126] showed the presence of linear and branched polymer chains in thermal polymerization of EA and *n*BA. One should note that NMR peaks corresponding to end-group substituents (ethyl and butyl) on each monomer unit can overlap with those of branch points on the polymer chain [60]. Electron spin (paramagnetic) resonance spectroscopy showed the existence of MCRs in free-radical polymerization [38,63,126].

An MCR formed by a backbiting reaction can participate in a β-scission reaction, leading to the formation of a secondary propagating radical (SPR) and a macromonomer (a dead polymer chain with a terminal double bond). Fig. 5.23 shows two possible pathways for the MCR fragmentation in a β-scission reaction. It was reported that the macromonomer can react with a radical and form a SPR; [127] at high temperatures β-scission reactions are more prevailing [1,10,128,129] and can produce highly uniform macromonomers [10]; and a balance between chain transfer and β-scission reactions may cause the formation of highly uniform macromonomers in high-temperature spontaneous (no initiator used) polymerization of *n*BA [128,129]. It was hypothesized that SPRs generated in β-scission reactions can further undergo backbiting reactions [128], further decreasing the polymer average chain length, favoring the formation of more MCRs and macromonomers, and facilitating the formation of uniform-chain-distribution polymer chains. It was also found experimentally that hydrogen bonding has a disruptive effect on acrylate backbiting mechanisms, so the level of branching depends of the nature of the solvent used [130].

The rate coefficients of various reactions in radical polymerization of acrylates were estimated from experimental measurements such as monomer conversion, average molecular weights, and branching level, using macroscopic-scale mechanistic models [13,34,73,74,77,131–133]. In thermal polymerization of *n*BA, the pre-exponential factor and activation energy were reported to be $(4.8-7.4)\times10^{7}$ s^{-1} and (31.7–32.7) kJ mol^{-1} for backbiting reactions and $(1.49\pm0.28)\times10^{9}$ s^{-1} and (63.9 ± 0.9) kJ mol^{-1} for β-scission [34,77,134]. The reliability of this estimation approach depends on the reliability of experimental measurements and the accuracy of the macroscopic-scale model used in the parameter estimation.

5.5.2 Knowledge Gained Using Quantum Chemical Calculations

Backbiting and β-scission reactions of acrylates have been studied using DFT methods in recent years [54,56,135]. Yu et al. [54] studied the 1:5 backbiting reactions of MA and *n*BA using UB3LYP/6−31G** (MPWB1K/6−31G**) level of theory and predicted an activation energy of 52.58 (59.94) kJ mol^{-1} and a frequency factor of 4.27×10^{12} (1.26×10^{13}) s^{-1} for MA (*n*BA). Liu et al. [135] studied several types of backbiting reactions in MA using the B3LYP, M06-2X and PBE0 density functionals and the 6−31G* basis set. Their study revealed that 1:5 backbiting mechanism with a six-membered ring transition state and 1:7 backbiting with an eight-membered ring transition state are kinetically more favorable than 1:3 backbiting and 1:9 backbiting. Cuccato et al. [55] investigated backbiting and β-scission reactions in *n*BA and found that 1:5 backbiting is the most favored mechanism. They also studied backbiting, propagation, and β-scission reactions in a terpolymer system of MA, styrene, and MMA [56]. DFT−predicted activation energies and frequency factors for 1:5 backbiting reactions reported in [54−56,135] are larger than the estimates obtained from experimental measurements using macroscopic-scale mechanistic models [34,77,134]. However, the DFT-predicted rate coefficients are in reasonable agreement with those estimated from measurements. These studies indicated that higher levels of theory should be applied to identify the source(s) of the reported discrepancies.

The rest of this chapter puts into perspective advances reported by Liu et al. [48], who modeled several mechanisms of backbiting and β-scission reactions in free-radical polymerization of MA using different levels of theory, and the RRHO and HR approximations. In particular, they studied backbiting and β-scission reaction mechanisms in self-initiated polymerization of MA using G4(MP2)-6X, DFT, and MP2 methods. They investigated the four types of intramolecular hydrogen transfer reactions, 1:3, 1:5, 1:7, and 1:9 backbiting, shown in Fig. 5.24. Each secondary live polymer chain undergoing backbiting is assumed to be initiated by the dimeric monoradical $M_2^{\bullet}$ (DMR) or the monomeric monoradical $M_1^{\bullet}$ (MMR). Liu et al. [48] also conducted a benchmarking study to identify the most cost-effective computational method(s) for studying the reactions and to assess the effects of different factors (e.g., functional type and chain length) on the reaction kinetic parameters, and then identify the most likely mechanisms with first-principles thermodynamic calculations and NMR spectra calculations. B3LYP, M06−2X, and PBE0 density functionals were used in the benchmark study. The objective was to benchmark the performance (in terms of energy barrier values calculated for backbiting and β-scission reactions) of several methods against G4(MP2)-6X, by calculating the energy barrier of a representative backbiting reaction with G4(MP2)-6X, MP2, and DFT [48]. The HR and harmonic oscillator (HO) approximations were used and also compared in the benchmark study. The composite quantum chemistry method G4(MP2)-6X [136,137] combines high-level calculations (e.g., CCSD(T) with the complete basis set) and less-expensive low-level calculations. As B3LYP was used widely in chemistry and is considered a standard

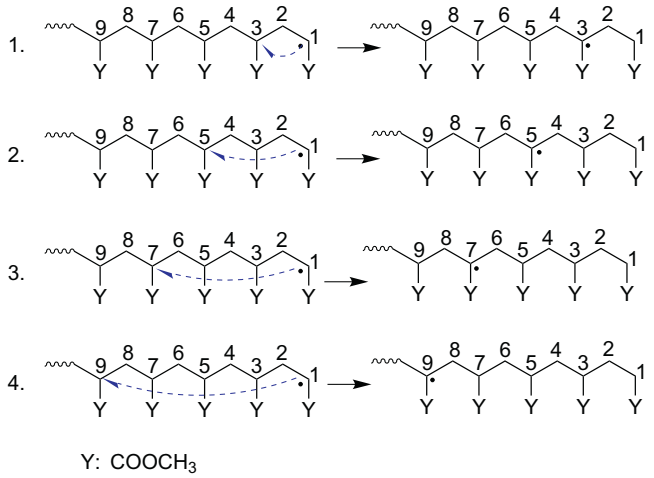

Figure 5.24
Various intramolecular hydrogen transfer reactions of a SPR in polymerization of MA. (1) 1:3 Backbiting, (2) 1:5 Backbiting, (3) 1:7 Backbiting, and (4) 1:9 Backbiting. *Reprinted with permission from S. Liu, S. Srinivasan, M.C. Grady, M. Soroush, A.M. Rappe, Backbiting and beta-scission reactions in free- radical polymerization of methyl acrylate, Int. J. Quantum Chem. 114 (2014) 345–360. Copyright 2014 American Chemical Society.*

functional [138], it was used to study these secondary reactions. M06-2X is a hybrid meta-density functional, which incorporates kinetic-energy density in both the exchange and correlation functionals, and also has fitted weights [81,139]. M06–2X has been shown to predict accurate rate constants for free-radical propagation reactions of acrylates. Liu et al. [48]. performed the G4(MP2)-6X calculations using Gaussian 09 [140] to take advantage of a parallel algorithm of open-shell CCSD(T) calculations. The rotational potential was scanned with 12 sampling points, which was found to be adequate to capture the features of the energy profiles [141,142]. All other calculations were carried out using GAMESS [143]. Hessian calculations were performed to determine the vibrational frequencies of reactants, products, and transition states. Vibrational frequency scaling factors were applied [138]. As the tunneling effect becomes important for hydrogen transfer reaction [144], the Eckart tunneling correction [145] was applied to compute the rate coefficients for the hydrogen transfer reactions based on transition-state theory [146]. The Wigner tunneling correction method [147] was applied to β-scission reactions. Details on the Eckart and Wigner corrections can be found in [89].

5.5.2.1 Benchmarking study of the 1:5 backbiting reaction

5.5.2.1.1 Composite method versus DFT and MP2

The 1:5 backbiting reaction of an MMR-initiated three-monomer unit SPR (denoted by 3MSPR) shown in Fig. 5.25A was chosen as the representative reaction for the benchmark

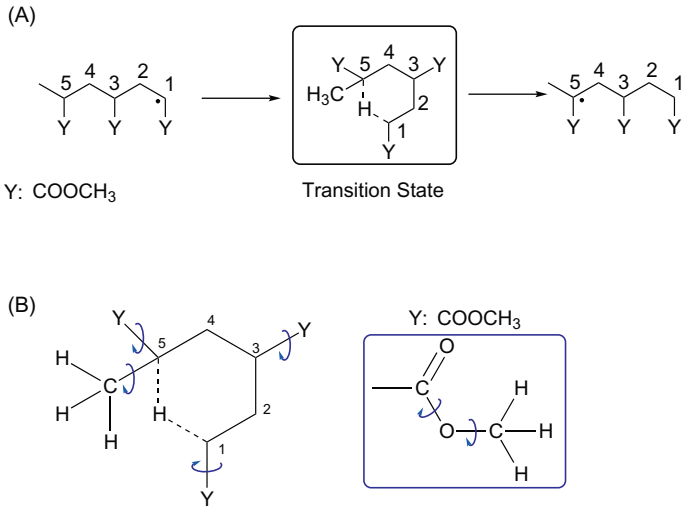

Figure 5.25

(A) The 1:5 backbiting reaction of 3MSPR for the benchmarking study. (B) Rotational axes of hindered rotors in the 1D-HR approximation. *Reprinted with permission from S. Liu, S. Srinivasan, M.C. Grady, M. Soroush, A.M. Rappe, Backbiting and beta-scission reactions in free- radical polymerization of methyl acrylate, Int. J. Quantum Chem. 114 (2014) 345–360. Copyright 2014 American Chemical Society.*

comparison of the composite method versus DFT and MP2. Electronic energy barriers calculated with G4(MP2)-6X, B3LYP/6−31G*, M06-2X/6−31G*, PBE0/6−31G* and MP2/6−31G* indicated that the barrier height estimated with B3LYP/6−31G* is the closest to that of G4(MP2)-6X, with an absolute percentage deviation (APD) of 7.0%, followed by M06-2X/6−31G* (APD = 7.2%), MP2/6−31G* (APD = 9.4%), and PBE0 (APD = 14.7%) [48]. B3LYP/6−31G* underestimated the barrier, and M06-2X/6−31G* overestimated the barrier relative to that of G4(MP2)-6X. This trend is opposite to that observed for radical propagation of MA, where B3LYP predicts a larger barrier than M06-2X [148]. This suggests that the large amount of exact exchange in M06-2X (54% HF exchange) may have different influence on addition and transfer reactions. As B3LYP and M06-2X performed equally well for backbiting reactions, these functionals were selected for the remaining studies [48]. Although PBE0/6−31G* predictions deviated most from those of G4(MP2)-6X, this functional was still used to understand its performance for large polymers.

5.5.2.1.2 HO versus HR

Fig. 5.25B shows internal rotations of all single bonds in the transition-state structure for the 1:5 backbiting reaction of 3MSPR. It is worth mentioning that the sigma bonds of the six-membered ring structure cannot rotate. Liu et al. [48] treated ten low-frequency modes in the initial propagating radical and the transition state as HRs. Using the 1D-HO

approximation, they calculated the activation entropy to be -10.0 J mol^{-1} K^{-1} and the frequency factor 5.11×10^{12} s^{-1}, and using the HR approximation -3.0 J mol^{-1} K^{-1} and 1.18×10^{13} s^{-1}. These predicted frequency factors are comparable to the values that Yu and Broadbelt [54] calculated for MA and *n*BA using the HR approximation. The difference of factor of ~ 2 between the predictions made using the HO and HR approximations implies that the less expensive but more accurate HO approximation can be used to calculate reliably rate coefficients of reactions in polymerization of alkyl acrylates.

5.5.2.2 Quantum chemistry versus laboratory experiments

No experimental value (obtained from laboratory experiments) for the rate coefficient of the 1:5 backbiting reaction of MA was reported. On the other hand, the 1:5 backbiting reaction rate coefficient of MA is believed to be close to that of *n*BA [54,121]. This motivated a comparison of Arrhenius parameter values of the 1:5 backbiting reaction of MA obtained using quantum chemistry methods to experimental values of the same parameters reported for *n*BA. Both G4(MP2)-6X and DFT-calculated values of the activation energy of the MA reaction are about 28 kJ mol^{-1} higher than the experimental value of the same parameter for *n*BA, whereas the frequency factor estimated with the HR approximation ($\sim 10^{12}$ s^{-1}) is about five orders of magnitude higher than the experimental value of the same parameter for *n*BA. However, in terms of reaction rate coefficient at room *T*, these theoretical and experimental values are surprisingly in reasonable agreement. Furthermore, these findings are in agreement with those reported by Yu et al. [54] and Cuccato et al. [55,56]. It appears that even the use of the high quality electronic structure calculation method (G4(MP2)-6X) and a sophisticated entropy calculation approach (HR approximation) does not result in eliminating the discrepancy between the theoretical and experimental values of the activation energy and frequency factor. The fact that the DFT-estimated rate constant agrees with the experimental value is attributed to the large error cancellation in electronic structure and entropy calculations when studying liquid-phase reactions in the gas-phase [149]. However, the origin of such a large error cancellation is not clear. Therefore, while it is legitimate to perform first-principles calculations in the gas-phase for reactions actually occurring in liquid-phase (given the good performance of DFT in predicting rate constants), further computational studies using a more realistic model (including solvation model) and a more accurate method for entropy calculations in liquid phase are still required.

5.5.2.3 Backbiting reactions of dimetric monoradical–initiated Live polymer chains

Liu et al. [48] studied the 1:3 and 1:5 backbiting reactions for a DMR-initiated four-monomer unit secondary radical (4DSPR), 1:3, 1:5, and 1:7 backbiting reactions for a DMR-initiated five-monomer unit secondary radical (5DSPR), and 1:3, 1:5, 1:7, 1:9 backbiting reactions for a DMR-initiated six-monomer unit secondary radical (6DSPR), as shown in Fig. 5.26. The transfer of a hydrogen atom (H_t) from the mid-chain carbon atoms C3, C5, C7, and C9 to the terminal carbon (C1) corresponds to 1:3, 1:5, 1:7, 1:9 backbiting

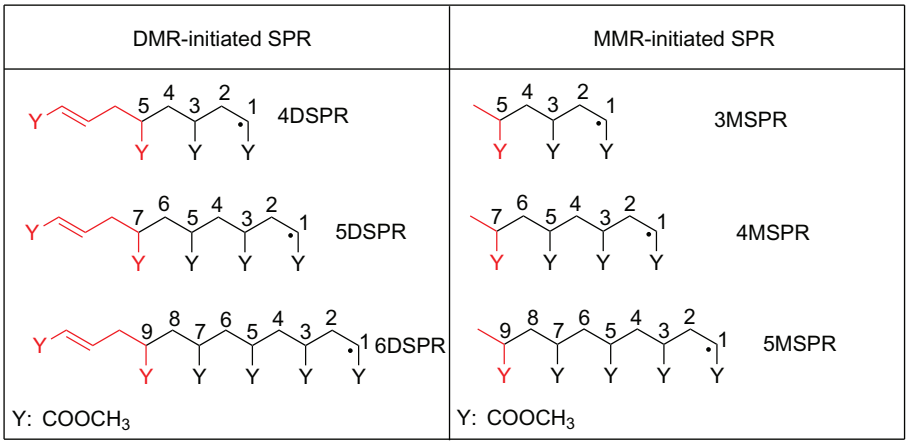

Figure 5.26
Structures of SPRs studied in this work. The initiator-end is colored red. *Reprinted with permission from S. Liu, S. Srinivasan, M.C. Grady, M. Soroush, A.M. Rappe, Backbiting and beta-scission reactions in free- radical polymerization of methyl acrylate, Int. J. Quantum Chem. 114 (2014) 345–360. Copyright 2014 American Chemical Society.*

mechanisms, respectively. An exploration of the potential energy surface by choosing r_1(C1-H_t) and r_2(Cn-H_t) for 1:n backbiting ($n = 3, 5, 7, 9$) as reaction coordinates, suggested that the geometry optimization is not appreciably affected by the change in density functional. It also indicated that (1) the size of basis set has little influence on the estimated thermodynamics constants, and (2) the 1:5 and 1:7 backbiting reactions are more energetically favored than 1:3 and 1:9 backbiting reactions [48]. All three levels of theory predicted that the energy barrier for 1:5 is comparable to that of the 1:7 backbiting mechanism for 6DSPR, with 1:3 and 1:9 considerably higher. The energy barrier of the 1:5 mechanism is lower than that of 1:7 in 5SPDR. This suggested that the chain length may have an influence on the type of backbiting mechanism that is most likely to occur; the longer 6DSPR chain allows the radical center to achieve the desired orientation by coiling itself to undergo 1:7 hydrogen transfer reaction. This agrees with experimental reports that have shown the presence of remote backbiting in thermal polymerization of alkyl acrylates, using electron paramagnetic resonance spectroscopy [126].

5.5.2.4 Backbiting reactions of monometic monoradical–initiated live polymer chains

Backbiting reactions of MMR-initiated SPRs with a chain length of three to five monomer units were explored using B3LYP, PBE0 and M06-2X/6-31G* (Fig. 5.26). The 1:3 and 1:5 backbiting mechanisms were investigated for the three-monomer unit live chain 3MSPR, the 1:3, 1:5, 1:7 backbiting mechanisms for an MMR-initiated four-monomer unit secondary radical (4MSPR), and the 1:3, 1:5, 1:7, 1:9 backbiting mechanisms for an MMR-initiated five-monomer unit secondary radical (5MSPR) [48]. The results again

indicated that the geometries of the transition-state structures using different levels of theory are similar. The highest activation energy was obtained using M06-2X/6−31G*, and the lowest using PBE0/6−31G*. Also, the use of a different basis set, 6−31G**, led to a similar finding; that is, the geometries of the identified of transition state structures are similar, and the calculated activation energies have the same trend but larger differences. The 1:5 and 1:7 backbiting mechanisms are more kinetically favored than the 1:3 and 1:9 backbiting ones. M06-2X/6−31G* predicted a higher activation energy, but PBE0/6−31G* a lower activation energy, in comparison to B3LYP/6-31−G*. The 1:5 mechanism has a lower energy barrier than the 1:7 one for 5MSPRs, which is comparable to the earlier findings by Liu et al. [48] for 5DSPRs. These results indicated that the type of initiating species does not influence the kinetics of backbiting reactions for live chains with the same polymer chain length (e.g., 5DSPR and 5MPR). The Mulliken charge analysis indicated little variation in electron density of the transfer center (tertiary carbon) with the type of initiating groups (DMR and MMR).

5.5.2.5 Effects of side chains

Yu et al. [54] studied the 1:5 backbiting of MA and *n*BA with a four-monomer polymer chain. Cuccato et al. [55] studied four types of backbiting reactions of *n*BA with a simplified molecular model in which the side chains of monomer units were replaced with hydrogen atoms except those (e.g. C1 and C5 for 1:5 backbiting reaction) directly participating in the hydrogen transfer. A comparison of the transition-state structures and kinetic constants calculated by Liu et al. [48] and by Yu et al. (using full atomic models) to those obtained by Cuccato et al. using a simplified model indicate that the side chains have no significant impact on either the located transition-state geometry or rate coefficients for the 1:5 backbiting reaction. The differences in the reaction coordinates were within 0.05 Å, the activation energies were similar [53 kJ mol^{-1} (Yu et al.), 50 kJ mol^{-1} (Liu et al. for 4MSPR), and 55 kJ mol^{-1} (Cuccato et al.)], and the rate constants were of the same order of magnitude. However, the rate constants for 1:7 and 1:9 backbiting reactions obtained using the complete molecular model were 3−4 orders of magnitude higher than those obtained using the simplified model [55]. This is due to larger frequency factors predicted by the complete molecular model that accounts for the side chains. It is probable that the substitution of side chains with hydrogen atoms in the simplified model leads to underestimating the entropy changes for those long-range hydrogen transfer reactions involving a large change of polymer conformations. This is the common trade-off between model simplicity and model-prediction accuracy. In addition, the comparable rate constant values reported by Liu et al. [48], Yu et al. [54], and Cuccato et al. [55] indicate that the type of initiating radical [self-initiation (DMR and MMR) versus external (peroxide/azonitrile)] does not influence the backbiting mechanisms.

5.5.2.6 β-Scission reactions of midchain radicals

Liu et al. [48] considered the two cleavage mechanisms: right (R)-side β-scission [which produces a macromonomer (dead polymer chain) including one of the two initiating groups] and left (L)-side β-scission (which produces a SPR including one of the two initiating groups), shown in Fig. 5.27. The β-scission reactions were explored using two reaction coordinates: the bond length of the σ bond (one carbon away from the radical site) to be broken, and the bond length of the double bond to be formed. The computational results indicated that the four-monomer unit DMR-initiated MCRs ($4DMCR^5$) and three-monomer unit MMR-initiated MCRs ($3MMCR^5$) can only undergo R-side β-scission, as the L-side β-scission produces an allene that is energetically unstable [48]. This suggested that the R-side β-scission is dominant for short-chain MCRs. The study showed that the molecular geometries are insensitive to the functional, which agrees with previous findings for backbiting reactions described in the previous sections. Both M06-2X and PBE0 predicted consistently higher energy barriers than B3LYP. Energy barriers obtained with M06-L/6-31G*, M06/6-31G*, and M06-2X/6-31G* (respectively, 108.7, 119.5, and 127.4 kJ mol^{-1}) indicated that a functional with a larger amount of exact exchange tends to predict a higher energy barrier. The different functionals indicated that the R-side and L-side β-scission have comparable energy barriers [48]. The length of the live polymer chain did not affect the energy barrier significantly. This can be attributed to the bond cleavage and formation in β-scission reactions occurring locally, with little change in the overall conformation of the polymer chain. Liu et al. [48] calculated β-scission rate constants using B3LYP/6-31G* and reported the constants to be around 10^{-4} s^{-1}, which agrees reasonably well with experimental and theoretical results reported in [13,56]. They reported that rate constants of some types of β-scission reactions are 1−2 orders of magnitude higher or lower than 10^{-4} s^{-1}, which is probably due to the dedicated intermolecular interactions between two fragments after cleavage. This may be a result of overestimation of the effect of the intermolecular interactions in gas-phase calculations. Further research using a solvation model may help identify the origin of restarted/facilitated β-scission reactions.

5.5.2.7 Calculated versus experimental nuclear magnetic resonance spectra

Liu et al. [48] calculated ^{13}C-NMR chemical shifts of the products of the backbiting and β-scission reactions. Fig. 5.28 depicts the predicted molecular structures and chemical shifts of the polymer chains formed by the backbiting reactions of a DMR-initiated five-monomer unit secondary radical (5DSPR) and an MMR-initiated four-monomer unit secondary radical (4MSPR). The 4MSPR-MMR and 5DSPR-MMR denote linear dead polymer chains generated by the termination-by-combination reaction of the 4MSPR and the MMR and by the same reaction of the 5DSPR and the MMR, respectively. Liu et al. [48] considered the three possible branched dead polymer chains formed by termination-by-combination reactions of: (1) the 3-position MCR and the MMR ($5DMCR^3$-MMR), (2) the 5-position

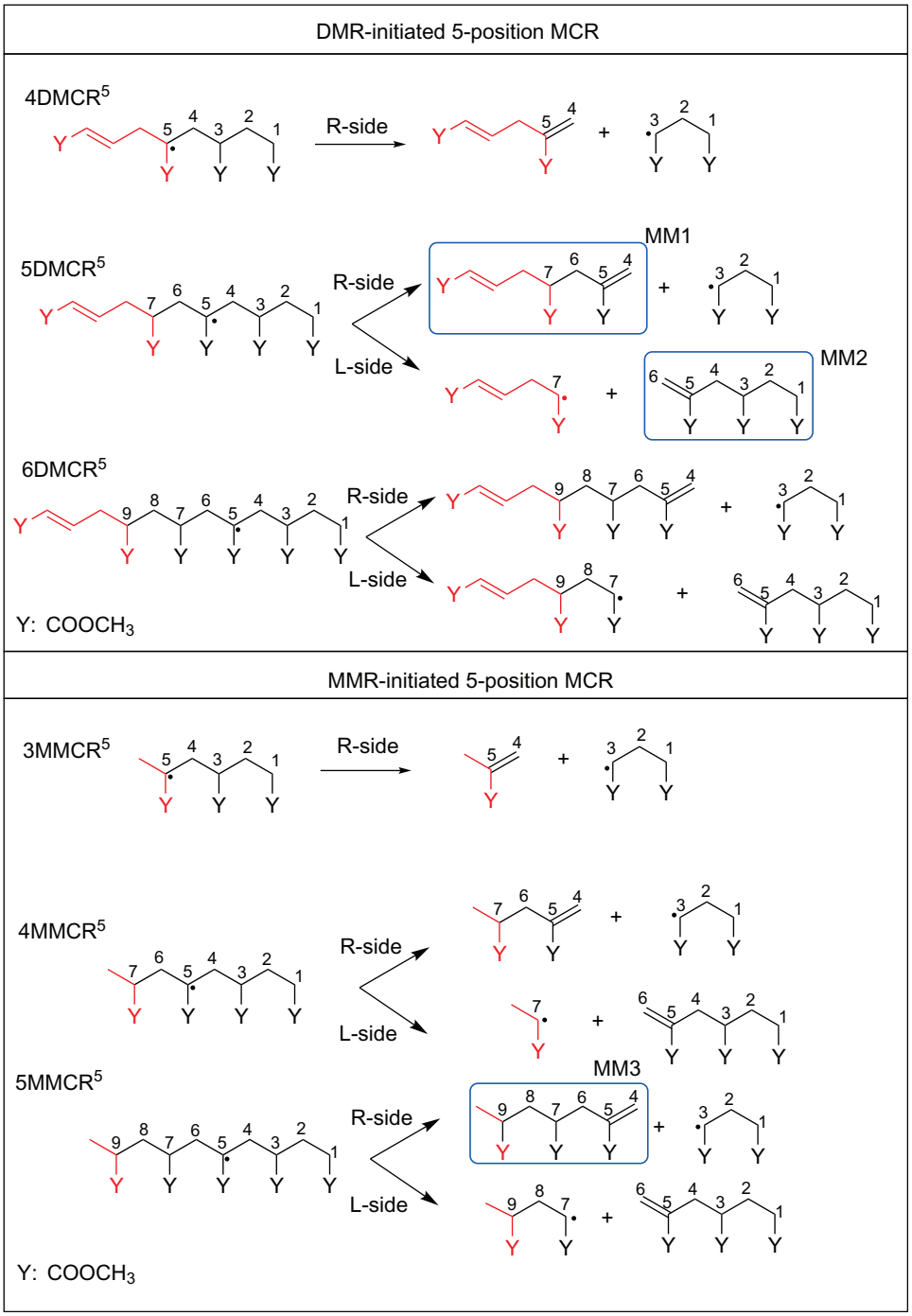

Figure 5.27

β-scission reactions from DMR-initiated MCRs and MMR-initiated MCRs. The initiator-end is colored red. *Reprinted with permission from S. Liu, S. Srinivasan, M.C. Grady, M., Soroush, A.M. Rappe, Backbiting and beta-scission reactions in free- radical polymerization of methyl acrylate, Int. J. Quantum Chem. 114 (2014) 345–360. Copyright 2014 American Chemical Society.*

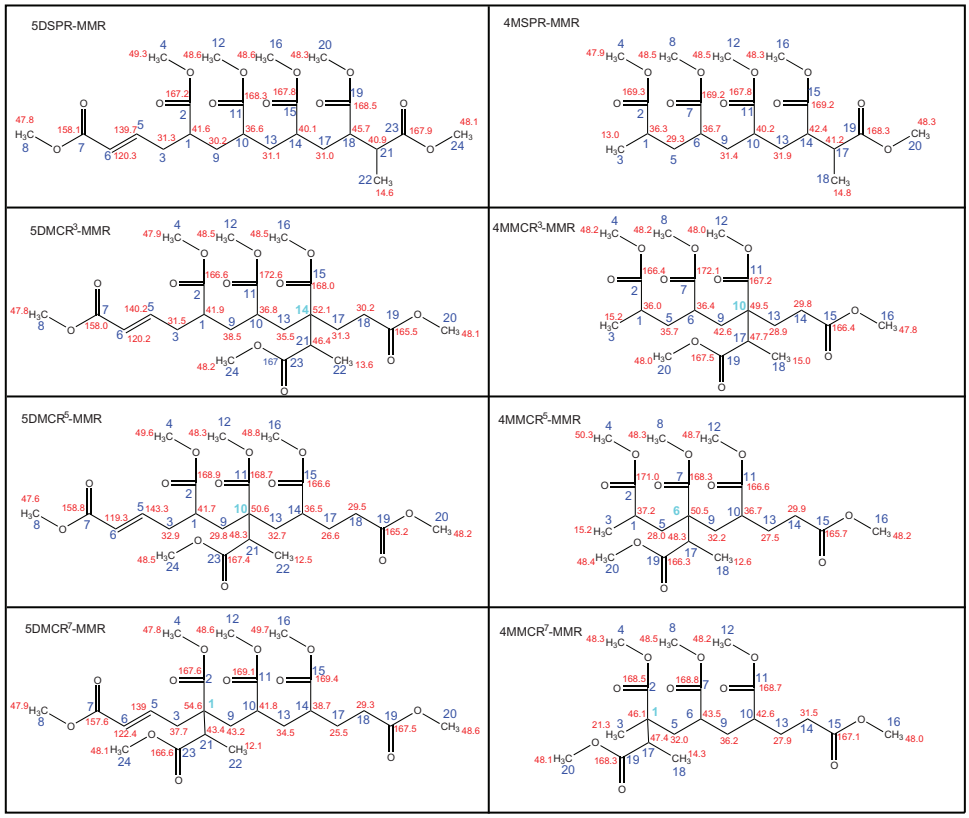

Figure 5.28

Calculated chemical shifts of C nucleus in linear and branched polymers of MA. *Reprinted with permission from S. Liu, S. Srinivasan, M.C. Grady, M. Soroush, A.M. Rappe, Backbiting and beta-scission reactions in free- radical polymerization of methyl acrylate, Int. J. Quantum Chem.114 (2014) 345–360. Copyright 2014 American Chemical Society.*

MCR and the MMR (5DMCR^5-MMR), and (3) the 7-position MCR and the MMR (5DMCR^7-MMR). Similarly, 4MMCR^3-MMR, 4MMCR^5-MMR, and 4MMCR^7-MMR represent dead polymer chains formed by termination-by-combination reactions of the 4MMCR and the MMR. Liu et al. [48] also calculated the ^{13}C-chemical shifts of the three macromonomers MM1, MM2 and MM3, shown in Fig. 5.27, where MM1 and MM3 are formed by the R-side β-scission reactions and MM2 by the L-side β-scission reaction. Figs. 5.29 and 5.30 depict the calculated ^{1}H and ^{13}C-NMR spectra of the three macromonomers. A comparison of the calculated chemical shifts to the experimental values reported by Quan et al. [14] showed that the calculated and experimental chemical shifts are comparable for various functional groups on the polymer backbone, side chain, and branches [48]. This indicated that B3LYP/6–31G* is a cost-effective method to predict the NMR chemical shifts of polymer chains of MA. These findings agree with previous studies

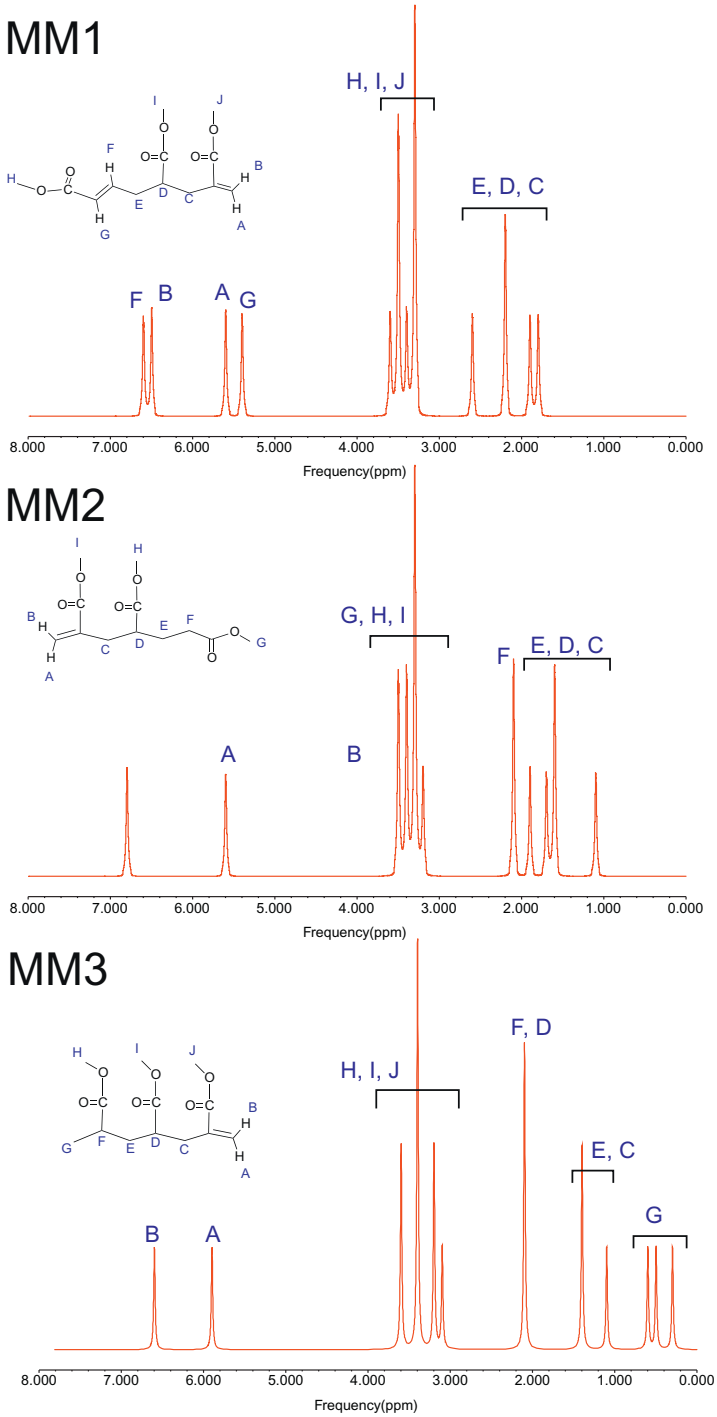

Figure 5.29

Simulated ^{1}H-NMR spectrums of selected macromonomers using B3LYP/6−31G*. *Reprinted with permission from S. Liu, S. Srinivasan, M.C. Grady, M. Soroush, A.M. Rappe, Backbiting and beta-scission reactions in free-radical polymerization of methyl acrylate, Int. J. Quantum Chem. 114 (2014) 345−360. Copyright 2014 American Chemical Society.*

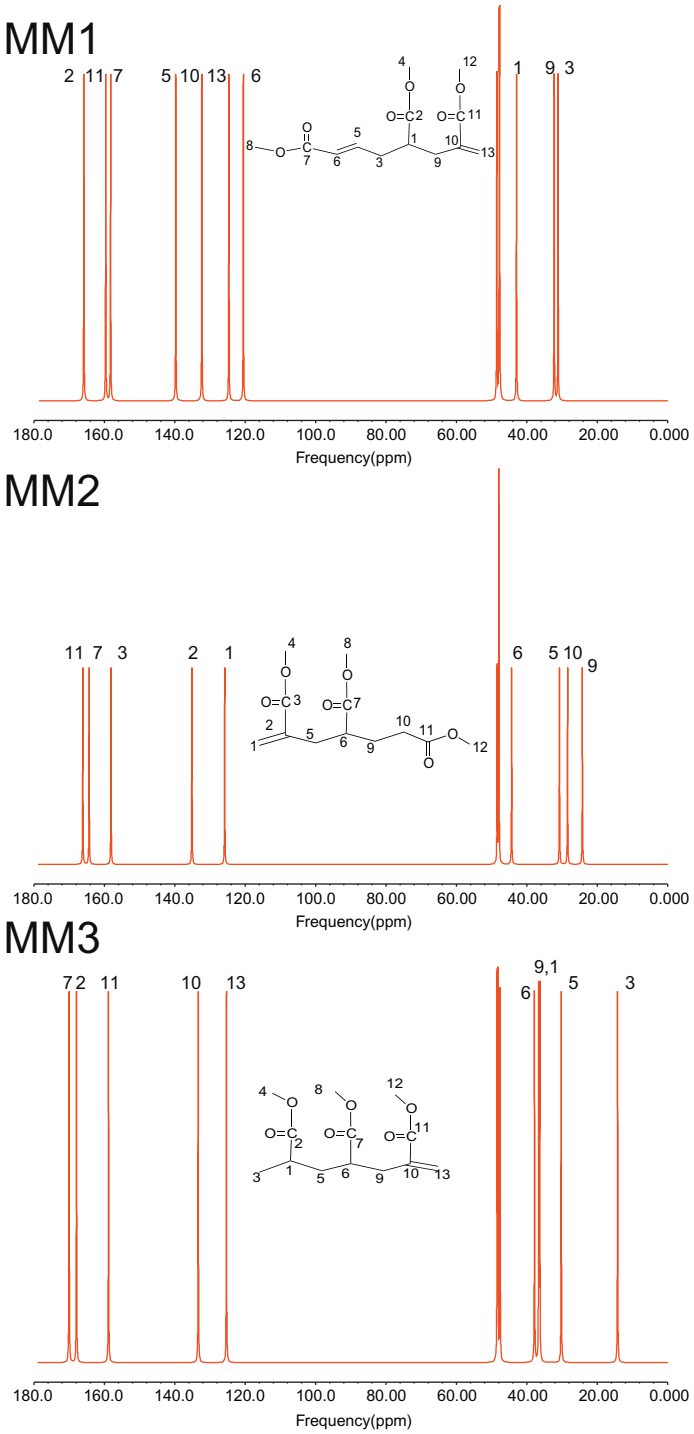

Figure 5.30

Simulated ^{13}C-NMR spectrums of selected macromonomers using B3LYP/6−31G*. *Reprinted with permission from S. Liu, S. Srinivasan, M.C. Grady, M. Soroush, A.M. Rappe, Backbiting and beta-scission reactions in free-radical polymerization of methyl acrylate, Int. J. Quantum Chem. 114 (2014) 345−360. Copyright 2014 American Chemical Society.*

[150,151] in suggesting that relatively simple basis sets (e.g., 6−31G*) and hybrid functionals (e.g., WP04 and B3LYP) can predict chemical shifts with practically adequate accuracy. The range of the calculated chemical shifts with B3LYP/6−31G* was found to be slightly larger than that of the experiments.

Several studies [14,128] suggested that the presence of terminal vinyl carbons in polymer chains in high-temperature polymerization is primarily due to the occurrence of β-scission reactions. The ^{1}H NMR spectra of macromonomers calculated by Liu et al. [48] were consistent with reported experimental ^{1}H NMR spectra of polyacrylates synthesized at high temperatures, showing the characteristic pair resonances at ∼5.5 and ∼6.5 ppm from terminal vinylidene structures (hydrogens of MM1 labeled A and B in Fig. 5.29) [10,14]. Results by Liu et al. [48] indicated that hydrogens of MM1 labeled F and G in Fig. 5.29 that originated from the DMR have chemical shifts at 5.4 and 6.6 ppm, which are probably partly responsible for the observed multiple peaks near 5.5 and 6.5 ppm in experimental ^{1}H NMR spectra [10,14]. Quan et al. [14] assigned the peaks near 126.7−128.3 ppm in the ^{13}C-NMR spectra to vinyl carbons at the end of chain (similar to C13 and C10 in macromonomer MM1 shown in Fig. 5.30), and the peaks near 126.7−128.3 ppm (both downfield and upfield) to aromatic carbons. As shown in the simulated NMR spectrum of MM1 (Fig. 5.30), C13 (124.7 ppm) and C10 (132.4 ppm) are from the β-scission reactions, and the nearby peaks at 120.6 ppm and 139.8 correspond respectively to the unsaturated carbon atoms C6 and C5 of the DMR. These suggest that the peaks at 125.4−126.0 ppm and 137.7−137.9 ppm reported in the experimental NMR spectrum [14] can be from the unsaturated carbon atoms of the DMR. They also indicate that both DMR and β scission−produced live radicals can produce unsaturated chain-end carbons in the final product, which is in agreement with previous studies [11,100] and points to the ability of the DMR to initiate polymerization. The agreement of computational and experimental NMR spectra points to DMR-based monomer self-initiation, the propagation of the DMR, and β-scission reactions in high-temperature polymerization of MA. The work of Liu et al. [48] showed that the nature of the reacting species and underlying reaction mechanisms can be validated by calculating NMR spectra via DFT-based methods and comparing the calculated spectra to those obtained experimentally. Combining this approach with existing empirical substitute increment schemes can provide an improved understanding of chain distributions and transient species in polymerization systems.

5.5.3 Backbiting and β-Scission Summary

The study by Liu et al. [48] revealed that the energy barriers of backbiting reactions of MA predicted using B3LYP, M06-2X, and G4(MP2)-6X are comparable. The entropies calculated using the RRHO and HR approximations were also comparable. DFT calculations indicated that the 1:5 backbiting mechanism with a six-membered ring

transition state and 1:7 backbiting with an eight-membered ring transition state are more energetically favored than 1:3 backbiting and 1:9 backbiting. They also revealed that the 1:5 backbiting mechanism is the most likely mechanism for intramolecular hydrogen transfer. The kinetic favorability of hydrogen transfer reactions, such as 1:7 and 1:9 backbiting, increases as the length of the reactant live polymer chain increases. The activation energies and rate coefficients of the left and right β-scission reactions are nearly equal [48]. The agreement between the theoretically predicted and experimental ^{13}C and ^{1}H NMR chemical shifts of species generated in the backbiting and β-scission reactions provided other evidence pointing to the occurrence of the postulated mechanisms. Both R-side and L-side β-scission reactions of the MCRs generated by 1:5 backbiting were found to have comparable, polymer chain length−independent activation energies. The agreement between the NMR spectra calculated with B3LYP/6-31G* and experimentally obtained spectra helped validate the proposed mechanisms. Using G4(MP2)-6X, Liu et al. [48] predicted activation energies that were larger than those obtained via macroscopic scale modeling and laboratory experimentation. This finding suggested that these reactions should be studied with more realistic models that account for solvent effects, and with better reaction mechanism models.

5.6 Computational Studies of Polymerization Reactions in Solution (Liquid Phase)

The effects of solvent on a reaction can be categorized into three types [152]. First, a solvent can have a bulk polar effect, in which the solvent dielectric field tends to localize the electronic distribution of the solute. When the transition state has a higher dipole moment than the reactants, the solvent stabilizes the transition state to a greater extent and reduces the reaction barrier. This polar effect has been reported to be little or absent in free-radical polymerization [153,154]. Second, a solvent can interact with the solute through partially covalent interactions such as hydrogen bonding. When the magnitude of these interactions with reactants differs greatly from those with transition states, a large solvent effect occurs. A significant increase in the propagation-reaction rate coefficient due to hydrogen bonding between butyl methacrylate and *n*-butanol has been reported [154]. The propagation reaction rate of MMA in benzyl alcohol has been found to be 80% higher than in bulk polymerization [153]. Third, a solvent can participate in chemical reactions [89].

Various continuum models have been developed to describe the bulk solvent effect. Continuum models, such as the dielectric polarizable continuum model (D-PCM) [105,155] and COSMO [109,156], have been applied to study solvent effects on radical polymerization with mixed success. However, the continuum solvation models fail when the explicit solvent effect, such as hydrogen-bonding, contributes to the solvent effect significantly. This weakness can be addressed using effective fragment potential

(EFP)-based, quantum mechanical/molecular mechanics (QM/MM), molecular dynamics (MD) simulations. In this MD simulation method, each solvent molecule is replaced with a single fragment potential, while performing ab initio calculations on the chemically active part (radical reactions of interest) [157,158]. This method permits first principles–based calculation of the potential of mean force along reaction coordinates. Explicit solvent models based on EFP (EFP1 and EFP2) are obtained entirely from quantum-mechanical calculations, consisting of Coulomb, polarization, dispersion, and exchange repulsion terms, allowing for modeling solvent-solute specific interactions such as hydrogen bonding.

5.7 Conclusion

Computational quantum chemistry revealed that favorable mechanisms for CTM in MA, EA, and *n*BA homopolymerization are the abstraction of a methylene hydrogen by a live polymer chain from EA and *n*BA, and a methyl hydrogen from MA. M06-2X/6–31G(*d,p*) predicted reaction kinetic parameters closest to those estimated from polymer sample data. The agreement of NMR chemical shifts of dead polymer chains predicted theoretically with those obtained from NMR spectroscopic analysis of polymer samples provided additional evidence that the postulated CTM mechanisms actually occur in polymerization. Transition state geometries of the CTM reactions were found to be insensitive to the choice of functionals and basis sets. While the CTM activation energies and rate coefficients calculated with B3LYP/6–31G(*d*) did not change appreciably with the length of live polymer chains, those calculated with M06-2X/6–31G(*d,p*) were different for CTM reactions involving live chains with two and three monomer units. All MA, EA, and *n*BA live chains initiated by $M_2^{\bullet}$ and those initiated by $M_1^{\bullet}$ have similar hydrogen abstraction abilities, pointing to little influence of the self-initiating species on CTM reactions. Hydrogen abstraction by a tertiary radical has a much larger energy barrier than that by a secondary radical.

Computational quantum chemistry showed that the abstraction of an hydrogen atom from a tertiary carbon atom is the most favorable CTP mechanism in alkyl acrylates. The monoradical $M_2^{\bullet}$ is as reactive as $M_1^{\bullet}$ in MA CTP reactions. Basis sets (6–31G(*d*), 6–31G (*d,p*), 6–311G(*d*), and 6–311G(*d,p*)) predicted similar transition geometries for the CTP mechanisms, activation energies with a maximum difference of 10 kJ mol^{-1}, and rate constants with a maximum difference of two orders of magnitude. The end-substituent groups of the monomers have little effect on the energy barriers of the CTP reactions. While the application of IEF-PCM showed strong solvent effects on the kinetic parameters of the CTP reactions of MA, EA, and *n*BA in *n*-butanol, the application of COSMO indicated no such remarkable effects.

Quantum chemical calculations revealed that the abstraction of a hydrogen from the methylene group next to the oxygen atom in *n*-butanol, from the methylene group in MEK,

and from a methyl group in *p*-xylene by a live polymer chain are the most likely mechanisms of CTS reactions in MA, EA, and *n*BA. Among *n*-butanol, *sec*-butanol and *tert*-butanol, *tert*-butanol has the highest CTS energy barrier and the lowest rate constant. Chain transfer to *n*-butanol and *sec*-butanol reactions have comparable kinetic parameter values. The activation energy of the most likely chain transfer to *p*-xylene mechanism of a two-monomer unit live *n*BA polymer chain initiated by $M_2^{\bullet}$ calculated using M06-2X/6−31G(*d,p*) is close to those estimated from polymer sample measurements. The application of PCM resulted in remarkable changes in the kinetic parameters of the chain transfer to *n*-butanol. However, it had very little effect on the stability of the reactants and the transition states in chain transfer to MEK and *p*-xylene. COSMO predicted no solvent effect on the kinetic parameters of CTS reactions of MA, EA, or *n*BA. The length of a live polymer chain has very little effect on the activation energies and rate coefficients of CTS reactions that the live chain participate in. MA, EA, and *n*BA live chains initiated by $M_2^{\bullet}$ and $M_1^{\bullet}$ showed similar hydrogen abstraction abilities, indicating that the type of mono-radicals generated via self-initiation has little or no effect on the CTS reactivity of MA, EA, and *n*BA live polymer chains.

Computational quantum chemistry showed that the 1:5 backbiting mechanism with a six-membered ring transition state and 1:7 backbiting with an eight-membered ring transition state are more kinetically favored than 1:3 backbiting and 1:9 backbiting. Moreover, the live polymer-chain length may influence the kinetic favorability of remote hydrogen transfer reactions, such as 1:7 and 1:9 backbiting reactions. The size of a basis set has no significant effect on the predicted values. Both B3LYP and M06-2X were found to be suitable for calculating energy barriers of backbiting reactions. Frequency factors calculated using the HO and HR approximations differ by a factor of 2. The rate coefficient values predicted using computational quantum chemistry agree with (1) values obtained using macroscopic-scale modeling and sample measurements from laboratory experiments, and (2) values predicted via DFT calculations by other investigators [54−56]. The chemical shifts of carbon nuclei in various final products predicted using B3LYP/6−31G* were found to be comparable to those obtained from spectroscopic polymer sample analyses.

Quantum chemical calculations revealed that R-side and L-side β-scission reactions of MCRs generated by 1:5 backbiting have comparable activation energies that are not dependent on the length of the MCRs. The NMR spectra calculated with B3LYP/6−31G* agree with experimental results, which further validates the proposed mechanisms. The application of a high quality first-principles method, G4(MP2), resulted in activation energies greater than those estimated from laboratory measurements using macroscopic-scale models, suggesting a need for (1) further theoretical studies of these reactions using more realistic models including the solvent effect and (2) the refinement of reaction mechanism models.

Continuum models, such as D-PCM [105,155] and COSMO [156,159], have been applied to radical polymerization with mixed success. However, their predictions are not reliable when an explicit solvent effect, such as hydrogen-bonding, is appreciably present. This inadequacy of the continuum models can be addressed by using EFP-based QM/MM MD simulations [157,158], which allow for calculating the potential of mean force along reaction coordinates, using first principles.

Acknowledgment

This material is based upon work supported by the U.S. National Science Foundation under Grant Nos. CBET–1804285 and CBET–1803215. Any opinions, findings, and conclusions or recommendations expressed in this material are those of the authors and do not necessarily reflect the views of the National Science Foundation.

References

[1] M.C. Grady, W.J. Simonsick, R.A. Hutchinson, Studies of higher temperature polymerization of n-butyl methacrylate and n-butyl acrylate, Macromol. Symp. 182 (2002) 149–168.
[2] F.S. Rantow, M. Soroush, M.C. Grady, G.A. Kalfas, Spontaneous polymerization and chain microstructure evolution in high-temperature solution polymerization of n-butyl acrylate, Polymer. (Guildf). 47 (2006) 1423–1435.
[3] J. Barth, M. Buback, G.T. Russell, S. Smolne, Chain-length-dependent termination in radical polymerization of acrylates, Macromol. Chem. Phys. 212 (2011) 1366–1378.
[4] K. O'Leary, D. Paul, Copolymers of poly (n-alkyl acrylates): synthesis, characterization, and monomer reactivity ratios, Polymer. (Guildf). 45 (2004) 6575–6585.
[5] P.A. Mueller, J.R. Richards, J.P. Congalidis, Polymerization reactor modeling in industry, Macromol. React. Eng. 5 (2011) 261–277.
[6] Air Quality: definition of volatile organic compounds; exclusion of trans 1-chloro-3, 3-trifluoroprop-1-ene, Rule document issued U.S. EPA; ID: EPA-HQ-OAR-2012-0393-0022, Date Posted: Aug 28, 2013; CFR: 40 CFR Part 51; Federal Register Number: 2013-21014; <https://www.regulations.gov/document?D = EPA-HQ-OAR-2012-0393-0022 >.
[7] 42nd united states congress, U. S. C., 2010 edition, title 42—the public health and welfare, Chapter 85-Air Pollution Prevention and Control. U.S. Government Printing Office, <www.gpo.gov >.
[8] Committee on Energy and Commerce. U.S. House of Representatives, Compilation of selected acts within the jurisdiction of the Committee on Energy and Commerce. As amended through December 31, 2000. Environmental law. Clean Air Act, Title I–Air Pollution Prevention and Control; Part A–Air Quality and Emission Limitations, US Government Printing Office, Washington, DC 1 (2001) 195–200.
[9] K. Adamsons, G. Blackman, B. Gregorovich, L. Lin, R. Matheson, Oligomers in the evolution of automotive clearcoats: mechanical performance testing as a function of exposure, Prog. Org. Coat. 34 (1998) 64–74.
[10] J. Chiefari, J. Jeffery, R.T.A. Mayadunne, G. Moad, E. Rizzardo, S.H. Thang, Chain transfer to polymer: a convenient route to macromonomers, Macromolecules 32 (1999) 7700–7702.
[11] S. Srinivasan, M.W. Lee, M.C. Grady, M. Soroush, A.M. Rappe, Computational study of the self-initiation mechanism in thermal polymerization of methyl acrylate, J. Phys. Chem. A. 113 (2009) 10787–10794.
[12] S. Srinivasan, M.W. Lee, M.C. Grady, M. Soroush, A.M. Rappe, Self-initiation mechanism in spontaneous thermal polymerization of ethyl and n-butyl acrylate: a theoretical study, J. Phys. Chem. A 114 (2010) 7975–7983.

[13] A.N. Nikitin, R.A. Hutchinson, W. Wang, G.A. Kalfas, J.R. Richards, C. Bruni, Effect of intramolecular transfer to polymer on stationary free-radical polymerization of alkyl acrylates, 5-consideration of solution polymerization up to high temperatures, Macromol. React. Eng. 4 (2010) 691–706.
[14] C.L. Quan, M. Soroush, M.C. Grady, J.E. Hansen, W.J. Simonsick, High-temperature homopolymerization of ethyl acrylate and n-butyl acrylate: polymer characterization, Macromolecules 38 (2005) 7619–7628.
[15] A.N.F. Peck, R.A. Hutchinson, Secondary reactions in the high-temperature free radical polymerization of butyl acrylate, Macromolecules 37 (2004) 5944–5951.
[16] S. Srinivasan, G. Kalfas, V.I. Petkovska, C. Bruni, M.C. Grady, M. Soroush, Experimental study of the spontaneous thermal homopolymerization of methyl and n-butyl acrylate, J. Appl. Polym. Sci. 118 (2010) 1898–1909.
[17] Gilbert, R.G., *Emulsion Polymerization: A Mechanistic Approach*; Academic Pr, 1995.
[18] G. Odian, Principles of Polymerization, 1991, J. Wiley & Sons, New York, 1988.
[19] D.F. Sangster, J. Feldthusen, J. Strauch, C.M. Fellows, Measurement of transfer coefficients to monomer for n-butyl methacrylate by molecular weight distributions from emulsion polymerization, Macromol. Chem. Phys. 209 (2008) 1612–1627.
[20] D. Kukulj, T.P. Davis, R.G. Gilbert, Chain transfer to monomer in the free-radical polymerizations of methyl methacrylate, styrene, and a-methylstyrene, Macromolecules 31 (1998) 994–999.
[21] K.Y. van Berkel, G.T. Russell, R.G. Gilbert, Molecular weight distributions and chain-stopping events in the free-radical polymerization of methyl methacrylate, Macromolecules 38 (2005) 3214–3224.
[22] S. Maeder, R.G. Gilbert, Measurement of transfer constant for butyl acrylate free-radical polymerization, Macromolecules 31 (1998) 4410–4418.
[23] J. Chiefari, Y. Chong, F. Ercole, J. Krstina, J. Jeffery, T.P. Le, et al., Living free-radical polymerization by reversible addition—fragmentation chain transfer: the raft process, Macromolecules 31 (1998) 5559–5562.
[24] Le, T.; Moad, G.; Rizzardo, E.; Thang, S. *Pct Int. Appl. Wo 9801478 A1 980115*, Chem. Abstr, 1998; p 115390.
[25] R.T. Mayadunne, E. Rizzardo, J. Chiefari, Y.K. Chong, G. Moad, S.H. Thang, Living radical polymerization with reversible addition—fragmentation chain Transfer (raft polymerization) using dithiocarbamates as chain transfer agents, Macromolecules 32 (1999) 6977–6980.
[26] M.S. Donovan, A.B. Lowe, B.S. Sumerlin, C.L. McCormick, Water-soluble polymers part 85-raft polymerization of N, N-dimethylacrylamide utilizing novel chain transfer agents tailored for high reinitiation efficiency and structural control, Macromolecules 35 (2002) 4123–4132.
[27] C. Barner-Kowollik, T.P. Davis, J.P.A. Heuts, M.H. Stenzel, P. Vana, M. Whittaker, Rafting down under: tales of missing radicals, fancy architectures, and mysterious holes, J. Polym. Sci. A, Polym. Chem. 41 (2003) 365–375.
[28] C.J. Hawker, A.W. Bosman, E. Harth, New polymer synthesis by nitroxide mediated living radical polymerizations, Chem. Rev. 101 (2001) 3661–3688.
[29] K. Matyjaszewski, J. Xia, Atom transfer radical polymerization, Chem. Rev. 101 (2001) 2921–2990.
[30] G. Odian, Principles of Polymerization, third ed, John Wiley & Sons, Inc., New York, 1991, pp. 243–249.
[31] M.P. Stevens, In *Polymer Chemistry: An Introduction*, third ed, Oxford University Press, Inc., New York, 1999, pp. 180–183.
[32] S. Beuermann, D. Paquet, J. McMinn, R. Hutchinson, Determination of free-radical propagation rate coefficients of butyl, 2-ethylhexyl, and dodecyl acrylates by pulsed-laser polymerization, Macromolecules 29 (1996) 4206–4215.
[33] M. Busch, A. Wahl, The significance of transfer reactions in pulsed laser polymerization experiments, Macromol. Theory Simul. 7 (1998) 217–224.
[34] A.N. Nikitin, R.A. Hutchinson, M. Buback, P. Hesse, Determination of intramolecular chain transfer and midchain radical propagation rate coefficients for butyl acrylate by pulsed laser polymerization, Macromolecules 40 (2007) 8631–8641.

[35] T.P. Davis, K.F. O'Driscoll, M.C. Piton, M.A. Winnik, Copolymerization propagation kinetics of styrene with alkyl acrylates, Polym. Int. 24 (1991) 65–70.
[36] R.A. Lyons, J. Hutovic, M.C. Piton, D.I. Christie, P.A. Clay, B.G. Manders, et al., Pulsed-laser polymerization measurements of the propagation rate coefficient for butyl acrylate, Macromolecules 29 (1996) 1918–1927.
[37] S. Beuermann, M. Buback, Rate coefficients of free-radical polymerization deduced from pulsed laser experiments, Progr. Polym. Sci. 27 (2002) 191–254.
[38] B. Yamada, M. Azukizawa, H. Yamazoe, D.J.T. Hill, P.J. Pomery, Free radical polymerization of cyclohexyl acrylate involving interconversion between propagating and mid-chain radicals, Polym. (Guildf). 41 (2000) 5611–5618.
[39] C. Farcet, J. Belleney, B. Charleux, R. Pirri, Structural characterization of nitroxide-terminated poly(N-butyl acrylate) prepared in bulk and miniemulsion polymerizations, Macromolecules 35 (2002) 4912–4918.
[40] W. Wang, A.N. Nikitin, R.A. Hutchinson, Consideration of macromonomer reactions in N-butyl acrylate free radical polymerization, Macromol. Rapid. Commun. 30 (2009) 2022–2027.
[41] Rier, T.; Srinivasan, S.; Soroush, M.; Kalfas, G.A.; Grady, M.C.; Rappe, A.M. In *macroscopic mechanistic modeling and optimization of a self-initiated high-temperature polymerization reactor*, American Control Conference (ACC), 2011, IEEE: 2011; pp 3071-3076.
[42] S.C. Thickett, R.G. Gilbert, Transfer to "monomer" in styrene free-radical polymerization, Macromolecules 41 (2008) 4528–4530.
[43] J. Brandrup, E. Immergut, Polymer Handbook Ed, 1989.
[44] J.M. Asua, S. Beuermann, M. Buback, P. Castignolles, B. Charleux, R.G. Gilbert, et al., Critically evaluated rate coefficients for free-radical polymerization, 5, Macromol. Chem. Phys. 205 (2004) 2151–2160.
[45] P.A. Lovell, T.H. Shah, F. Heatley, Chain transfer to polymer in emulsion polymerization of N-butyl acrylate studied by carbon-13 Nmr spectroscopy and gel permeation chromatography, Polym. Commun. 32 (1991) 98–103.
[46] Lovell, P.; Shah, T.; Heatley, F. Polymer latexes, in: E.S. Daniels; E.D. Sudol, M.S. El-Aasser (Eds.), *Preparation, Characterization and Application,*, ACS Symposium Series, 1992, 188.
[47] N. Moghadam, S. Srinivasan, M.C. Grady, A.M. Rappe, M. Soroush, Theoretical study of chain transfer to solvent reactions of alkyl acrylates, J. Phys. Chem. A 118 (2014) 5474–5487.
[48] S. Liu, S. Srinivasan, M.C. Grady, M. Soroush, A.M. Rappe, Backbiting and β-scission reactions in free-radical polymerization of methyl acrylate, Int. J. Quantum. Chem. 114 (2014) 345–360.
[49] E. Mavroudakis, D. Cuccato, D. Moscatelli, Quantum mechanical investigation on bimolecular hydrogen abstractions in butyl acrylate-based free radical polymerization processes, J. Phys. Chem. A 118 (2014) 1799–1806.
[50] N. Moghadam, S. Liu, S. Srinivasan, M.C. Grady, A.M. Rappe, M. Soroush, Theoretical study of intermolecular chain transfer to polymer reactions of alkyl acrylates, Ind. Eng. Chem. Res. 54 (2015) 4148–4165.
[51] N. Moghadam, S. Liu, S. Srinivasan, M.C. Grady, M. Soroush, A.M. Rappe, Computational study of chain transfer to monomer reactions in high-temperature polymerization of alkyl acrylates, J. Phys. Chem. A 117 (2013) 2605–2618.
[52] M. Stevens, Polymer Chemistry. An Introduction, third ed., Oxford University Press, New York, 1999.
[53] N.M. Ahmad, F. Heatley, P.A. Lovell, Chain transfer to polymer in free-radical solution polymerization of n-butyl acrylate studied by NMR spectroscopy, Macromolecules 31 (1998) 2822–2827.
[54] X.R. Yu, L.J. Broadbelt, Kinetic study of 1,5-hydrogen transfer reactions of methyl acrylate and butyl acrylate using quantum chemistry, Macromol. Theory Simul. 21 (2012) 461–469.
[55] D. Cuccato, E. Mavroudakis, M. Dossi, D. Moscatelli, A. Density, Functional theory study of secondary reactions in N-butyl acrylate free radical polymerization, Macromol. Theory Simul. 22 (2013) 127–135.
[56] D. Cuccato, E. Mavroudakis, D. Moscatelli, Quantum chemistry investigation of secondary reaction kinetics in acrylate-based copolymers, J. Phys. Chem. A 117 (2013) 4358–4366.

[57] Y. Reyes, J.M. Asua, Revisiting chain transfer to polymer and branching in controlled radical polymerization of butyl Acrylate, Macromol. Rapid Commun. 32 (2011) 63−67.
[58] J.A. Rawlston, F.J. Schork, M.A. Grover, Multiscale modeling of branch length in butyl acrylate solution polymerization: molecular versus continuum kinetics, Macromol. Theory Simul. 20 (2011) 645−659.
[59] S.Y. Yu-Su, F.C. Sun, S.S. Sheiko, D. Konkolewicz, H.I. Lee, K. Matyjaszewski, Molecular imaging and analysis of branching topology in polyacrylates by atomic force microscopy, Macromolecules 44 (2011) 5928−5936.
[60] N.M. Ahmad, et al., Chain transfer to polymer and branching in controlled radical polymerizations of N-butyl acrylate, Macromol. Rapid Commun. 30 (2009) 2002−2021.
[61] J. Barth, M. Buback, C. Barner-Kowollik, T. Junkers, G.T. Russell, Single-pulse pulsed laser polymerization-electron paramagnetic resonance investigations into the termination kinetics of n-butyl acrylate macromonomers, J. Polym. Sci. A, Polym. Chem. 50 (2012) 4740−4748.
[62] B.C. Gilbert, J.R.L. Smith, E.C. Milne, A.C. Whitwood, P. Taylor, Kinetic and structural Epr studies of radical polymerization—monomer, dimer, trimer and midchain radicals formed via the initiation of polymerization of acrylic-acid and related-compounds with electrophilic radicals (center-dot-oh, So4 radical-ion and Cl2 radical-ion), J. Chem. Soc. Perkin. Trans. 2 (1994) 1759−1769.
[63] M. Azukizawa, B. Yamada, D.J.T. Hill, P.J. Pomery, Radical polymerization of phenyl acrylate as studied by Esr spectroscopy: concurrence of propagating and mid-chain radicals, Macromol. Chem. Phys. 201 (2000) 774−781.
[64] C. Plessis, G. Arzamendi, J.R. Leiza, H.A.S. Schoonbrood, D. Charmot, J.M. Asua, A decrease in effective acrylate propagation rate constants caused by intramolecular chain transfer, Macromolecules 33 (2000) 4−7.
[65] C. Plessis, G. Arzamendi, J.M. Alberdi, A.M. van Herk, J.R. Leiza, J.M. Asua, Evidence of branching in poly(butyl acrylate) produced in pulsed-laser polymerization experiments, Macromol. Rapid Commun. 24 (2003) 173−177.
[66] S. Santanakrishnan, L. Tang, R.A. Hutchinson, M. Stach, I. Lacik, J. Schrooten, et al., Kinetics and modeling of batch and semibatch aqueous-phase NVP free-radical polymerization, Macromol. React. Eng. 4 (2010) 499−509.
[67] C. Plessis, G. Arzamendi, J.R. Leiza, H.A.S. Schoonbrood, D. Charmot, J.M. Asua, Modeling of seeded semibatch emulsion polymerization of N-Ba, Ind. Eng. Chem. Res. 40 (2001) 3883−3894.
[68] M. Angoy, M.I. Bartolome, E. Vispe, P. Lebeda, M.V. Jimenez, J.J. Perez-Torrente, et al., Branched poly (phenylacetylene), Macromolecules 43 (2010) 6278−6283.
[69] S.D. Tobing, A. Klein, Molecular parameters and their relation to the adhesive performance of acrylic pressure-sensitive adhesives, J. Appl. Polym. Sci. 79 (2001) 2230−2244.
[70] N.M. Ahmad, D. Britton, F. Heatley, P.A. Lovell, Chain transfer to polymer in emulsion polymerization, Macromol. Symp. 143 (1999) 231−241.
[71] A.N. Nikitin, P. Castignolles, B. Charleux, J.P. Vairon, Simulation of molecular weight distributions obtained by pulsed laser polymerization (PLP): new analytical expressions including intramolecular chain transfer to the polymer, Macromol. Theory Simul. 12 (2003) 440−448.
[72] A.N. Nikitin, P. Castignolles, B. Charleux, J.P. Vairon, Determination of propagation rate coefficient of acrylates by pulsed-laser polymerization in the presence of intramolecular chain transfer to polymer, Macromol. Rapid Commun 24 (2003) 778−782.
[73] A.N. Nikitin, R.A. Hutchinson, The effect of intramolecular transfer to polymer on stationary free radical polymerization of alkyl acrylates, Macromolecules 38 (2005) 1581−1590.
[74] A.N. Nikitin, R.A. Hutchinson, Effect of intramolecular transfer to polymer on stationary free radical polymerization of alkyl acrylates, 2—improved consideration of termination, Macromol. Theory Simul. 15 (2006) 128−136.
[75] F. Heatley, P.A. Lovell, T. Yamashita, Chain transfer to polymer in free-radical solution polymerization of 2-ethylhexyl acrylate studied by NMR spectroscopy, Macromolecules 34 (2001) 7636−7641.
[76] G. Arzamendi, C. Plessis, J.R. Leiza, J.M. Asua, Effect of the intramolecular chain transfer to polymer on plp/sec experiments of alkyl acrylates, Macromol. Theory Simul. 12 (2003) 315−324.

[77] A.N. Nikitin, R.A. Hutchinson, G.A. Kalfas, J.R. Richards, C. Bruni, The effect of intramolecular transfer to polymer on stationary free-radical polymerization of alkyl acrylates, 3-consideration of solution polymerization up to high conversions, Macromol. Theory Simul. 18 (2009) 247–258.
[78] J.M. Asua, S. Beuermann, M. Buback, P. Castignolles, B. Charleux, R.G. Gilbert, et al., Critically evaluated rate coefficients for free-radical polymerization, 5—propagation rate coefficient for butyl acrylate, Macromol. Chem. Phys. 205 (2004) 2151–2160.
[79] C. Barner-Kowollik, F. Gunzler, T. Junkers, Pushing the limit: pulsed laser polymerization of n-butyl acrylate at 500 Hz, Macromolecules 41 (2008) 8971–8973.
[80] S. Haseebuddin, K. Raju, M. Yaseen, Applicability of the Wlf equation to polyurethane polyols and film properties of their resins, Prog. Org. Coat. 30 (1997) 25–30.
[81] Y. Zhao, D.G. Truhlar, The M06 suite of density functionals for main group thermochemistry, thermochemical kinetics, noncovalent interactions, excited states, and transition elements: two new functionals and systematic testing of four M06-class functionals and 12 other functionals, Theor. Chem. Acc. 120 (2008) 215–241.
[82] Y. Zhao, D.G. Truhlar, Density functionals with broad applicability in chemistry, Acc. Chem. Res. 41 (2008) 157–167.
[83] Y. Zhao, D.G. Truhlar, How well can new-generation density functionals describe the energetics of bond-dissociation reactions producing radicals?, J. Phys. Chem. A 112 (2008) 1095–1099.
[84] M.W. Schmidt, et al., General atomic and molecular electronic-structure system, J. Comput. Chem. 14 (1993) 1347–1363. Available at <http://www.msg.ameslab.gov/GAMESS/GAMESS.html>.
[85] R.X.E. Willemse, A.M. van Herk, E. Panchenko, T. Junkers, M. Buback, PLP-ESR monitoring of midchain radicals in N-butyl acrylate polymerization, Macromolecules 38 (2005) 5098–5103.
[86] M. Buback, P. Hesse, T. Junkers, T. Sergeeva, T. Theist, PLP labeling in ESR spectroscopic analysis of secondary and tertiary acrylate propagating radicals, Macromolecules 41 (2008) 288–291.
[87] Y. Zhao, N.E. Schultz, D.G. Truhlar, Design of density functionals by combining the method of constraint satisfaction with parametrization for thermochemistry, thermochemical kinetics, and noncovalent interactions, J. Chem. Theory Comput. 2 (2006) 364–382.
[88] Y. Zhao, N.E. Schultz, D.G. Truhlar, Exchange-correlation functional with broad accuracy for metallic and nonmetallic compounds, kinetics, and noncovalent interactions, J. Chem. Phys. (2005) 123.
[89] S. Liu, S. Srinivasan, M.C. Grady, M. Soroush, A.M. Rappe, Computational study of cyclohexanone-monomer co-initiation mechanism in thermal homopolymerization of methyl acrylate and methyl methacrylate, J. Phys. Chem. A 116 (2012) 5337–5348.
[90] S. Liu, S. Srinivasan, J. Tao, M.C. Grady, M. Soroush, A.M. Rappe, Modeling spin-forbidden monomer self-initiation reactions in spontaneous free-radical polymerization of acrylates and methacrylates, J. Phys. Chem. A 118 (2014) 9310–9318.
[91] K. Sharp, Entropy-enthalpy compensation: fact or artifact? Protein. Sci. 10 (2001) 661–667.
[92] X. Yu, J. Pfaendtner, L.J. Broadbelt, Ab initio study of acrylate polymerization reactions: methyl methacrylate and methyl acrylate propagation, J. Phys. Chem. A 112 (2008) 6772–6782.
[93] K. Liang, R.A. Hutchinson, J. Barth, S. Samrock, M. Buback, Reduced branching in poly(butyl acrylate) via solution radical polymerization in N-butanol, Macromolecules 44 (2011) 5843–5845.
[94] E.I. Izgorodina, M.L. Coote, Accurate ab initio prediction of propagation rate coefficients in free-radical polymerization: acrylonitrile and vinyl chloride, Chem. Phys. 324 (2006) 96–110.
[95] M. Buback, S. Klingbeil, J. Sandmann, M.B. Sderra, H.P. Vogele, H. Wackerbarth, et al., Pressure and temperature dependence of the decomposition rate of tert-butyl peroxyacetate and of tert-butyl peroxypivalate, Z. Phys. Chem. Int. J. Res. Phys. Chem. Chem. Phys. 210 (1999) 199–221.
[96] J.K. Song, J.W. van Velde, L.L.T. Vertommen, L.G.J. van der Ven, R.M.A. Heeren, O.F. van den Brink, Investigation of polymerization mechanisms of poly(n-butyl acrylate)S generated in different solvents by Lc-Esi-Ms2, Macromolecules 43 (2010) 7082–7089.
[97] P.V.T. Raghuram, U.S. Nandi, Studies on the polymerization of ethyl acrylate. II. Chain transfer studies, J. Polym. Sci. 7 (1969) 2379–2385.
[98] S.D. Gadkary, S.L. Kapur, Chain transfer in solution polymerization III. Methyl acrylate, Macromol. Chem. Phys. 17 (1955) 29–38.

[99] R. Jovanovic, M.A. Dube, Solvent effects in butyl acrylate and vinyl acetate homopolymerizations in toluene, J. Appl. Polym. Sci. 94 (2004) 871–876.
[100] S. Srinivasan, G. Kalfas, V.I. Petkovska, C. Bruni, M.C. Grady, M. Soroush, Experimental study of the spontaneous thermal homopolymerization of methyl and n-butyl acrylate, J. Appl. Polym. Sci. 118 (2010) 1898–1909.
[101] S. Beuermann, D.A. Paquet, J.H. McMinn, R.A. Hutchinson, Determination of free-radical propagation rate coefficients of butyl, 2-ethylhexyl, and dodecyl acrylates by pulsed-laser polymerization, Macromolecules 29 (1996) 4206–4215.
[102] T.P. Davis, K.F. Odriscoll, M.C. Piton, M.A. Winnik, Copolymerization propagation kinetics of styrene with alkyl acrylates, Polym. Int. 24 (1991) 65–70.
[103] Grady, M.C.; Quan, C.; Soroush, M. Thermally initiated polymerization process. U.S. Patent Application Number 60/484,393, filed on July 2, 2003.
[104] J.R. Pliego, J.M. Riveros, The cluster-continuum model for the calculation of the solvation free energy of ionic species, J. Phys. Chem. A 105 (2001) 7241–7247.
[105] S.C. Thickett, R.G. Gilbert, Propagation rate coefficient of acrylic acid: theoretical investigation of the solvent effect, Polymer. (Guildf). 45 (2004) 6993–6999.
[106] L. Onsager, Electric moments of molecules in liquids, J. Am. Chem. Soc. 58 (1936) 1486–1493.
[107] J. Tomasi, B. Mennucci, R. Cammi, Quantum mechanical continuum solvation models, Chem. Rev. 105 (2005) 2999–3093.
[108] R. Cammi, B. Mennucci, J. Tomasi, On the calculation of local field factors for microscopic static hyperpolarizabilities of molecules in solution with the aid of quantum-mechanical methods, J. Phys. Chem. A 102 (1998) 870–875.
[109] A. Klamt, G. Schuurmann, Cosmo—a new approach to dielectric screening in solvents with explicit expressions for the screening energy and its gradient, J. Chem. Soc. Perkin. Trans. 2 (1993) 799–805.
[110] K.X. Fu, Q. Zhu, X.Y. Li, Z. Gong, J.Y. Ma, R.X. He, Continuous medium theory for nonequilibrium solvation: iv. solvent reorganization energy of electron transfer based on conductor-like screening model, J. Comput. Chem. 27 (2006) 368–374.
[111] A. Klamt, Conductor-like screening model for real solvents: a new approach to the quantitative calculation of solvation phenomena, J. Phys. Chem. 99 (7) (1995) 2224–2235.
[112] P. Deglmann, I. Müller, F. Becker, A. Schäfer, K.D. Hungenberg, H. Weiß, Prediction of propagation rate coefficients in free radical solution polymerization based on accurate quantum chemical methods: vinylic and related monomers, including acrylates and acrylic acid, Macromol. React. Eng. 3 (2009) 496–515.
[113] http://Cccbdb.Nist.Gov/; Accessed 06/11/2010.
[114] R.J. McMahon, Chemical reactions involving quantum tunneling, Science 299 (2003) 833–834.
[115] E.P. Wigner, Calculation of the rate of elementary association reactions, J. Chem. Phys. 5 (1937) 720–725.
[116] http://En.Wikipedia.Org/Wiki/Bond-Dissociation_Energy (12/2012).
[117] A. Tkatchenko, M. Scheffler, Accurate molecular Van Der Waals interactions from ground-state electron density and free-atom reference data, Phys. Rev. Lett. 102 (2009) 073005.
[118] S. Grimme, J. Antony, S. Ehrlich, H. Krieg, A consistent and accurate ab initio parametrization of density functional dispersion correction (DFT-D) for the 94 elements H-Pu, J. Chem. Phys. 132 (2010) 154104.
[119] S. Ehrlich, J. Moellmann, W. Reckien, T. Bredow, S. Grimme, System-dependent dispersion coefficients for the DFT-D3 treatment of adsorption processes on ionic surfaces, Chemphyschem 12 (2011) 3414–3420.
[120] C. Barner-Kowollik, S. Beuermann, M. Buback, P. Castignolles, B. Charleux, M.L. Coote, et al., Critically evaluated rate coefficients in radical polymerization-7. Secondary-radical propagation rate coefficients for methyl acrylate in the bulk, Polym. Chem. 5 (2014) 204–212.
[121] T. Junkers, C. Barner-Kowollik, The role of mid-chain radicals in acrylate free radical polymerization: branching and scission, J. Polym. Sci. A, Polym. Chem. 46 (2008) 7585–7605.

[122] A.M. van Herk, Historic account of the development in the understanding of the propagation kinetics of acrylate radical polymerizations, Macromol. Rapid Commun. 30 (2009) 1964–1968.
[123] D. Britton, F. Heatley, P.A. Lovell, Chain transfer to polymer in free-radical bulk and emulsion polymerization of vinyl acetate studied by Nmr spectroscopy, Macromolecules 31 (1998) 2828–2837.
[124] D. Lim, O. Wichterle, Chain transfer of polymer in radical polymerization, J. Polym. Sci. 29 (1958) 579–584.
[125] M.J. Roedel, The molecular structure of polyethylene. 1. Chain branching in polyethylene during polymerization, J. Am. Chem. Soc. 75 (1953) 6110–6112.
[126] J. Barth, M. Buback, P. Hesse, T. Sergeeva, Epr analysis of N-butyl acrylate radical polymerization, Macromol. Rapid Commun. 30 (2009) 1969–1974.
[127] B. Yamada, F. Oku, T. Harada, Substituted propenyl end groups as reactive intermediates in radical polymerization, J. Polym. Sci. A, Polym. Chem. 41 (2003) 645–654.
[128] T. Junkers, F. Bennet, S.P.S. Koo, C. Barner-Kowollik, Self-directed formation of uniform unsaturated macromolecules from acrylate monomers at high temperatures, J. Polym. Sci. A, Polym. Chem. 46 (2008) 3433–3437.
[129] A.M. Zorn, T. Junkers, C. Barner-Kowollik, Synthesis of a macromonomer library from high-temperature acrylate polymerization, Macromol. Rapid Commun. 30 (2009) 2028–2035.
[130] K. Liang, R.A. Hutchinson, The effect of hydrogen bonding on intramolecular chain transfer in polymerization of acrylates, Macromol. Rapid Commun. 32 (2011) 1090–1095.
[131] A.N. Nikitin, R.A. Hutchinson, Effect of intramolecular transfer to polymer on stationary free radical polymerization of alkyl acrylates, 4-consideration of penultimate effect, Macromol. Rapid Commun. 30 (2009) 1981–1988.
[132] J.M. Asua, et al., Critically evaluated rate coefficients for free-radical polymerization, 5—propagation rate coefficient for butyl acrylate, Macromol. Chem. Phys. 205 (2004) 2151–2160.
[133] W. Wang, R.A. Hutchinson, Free-radical acrylic polymerization kinetics at elevated temperatures, Chem. Eng. Technol. 33 (2010) 1745–1753.
[134] J. Barth, M. Buback, P. Hesse, T. Sergeeva, Termination and transfer kinetics of butyl acrylate radical polymerization studied via Sp-Plp-Epr, Macromolecules 43 (2010) 4023–4031.
[135] S. Liu, S. Srinivasan, M.C. Grady, M. Soroush, A.M. Rappe, Understanding backbiting and beta-scission reactions in self-initiated polymerization of methyl acrylate: a theoretical study, 2012, AlChE, Pittsburgh, PA, 2012.
[136] B. Chan, J. Deng, L. Radom, G4(Mp2)-6x: a cost-effective improvement to G4(Mp2), J. Chem. Theory Comput. 7 (2011) 112–120.
[137] B. Chan, L. Radom, Bde261: a comprehensive set of high-level theoretical bond dissociation enthalpies, J. Phys. Chem. A 116 (2012) 4975–4986.
[138] K. Burke, Perspective on density functional theory, Phys. Chem. 136 (2012) 150901.
[139] Y. Zhao, D.G. Truhlar, How well can new-generation density functionals describe protonated epoxides where older functionals fail?, J. Org. Chem. 72 (2007) 295–298.
[140] Gaussian 09, R.A. Frisch, M.J. Trucks, G.W. Schlegel, H.B. Scuseria, G.E. Robb, M.A. Cheeseman, J.R. Scalmani, G. Barone, V. Mennucci, B. Petersson, G.A. Nakatsuji, H. Caricato, M. Li, X. Hratchian H.P.; Izmaylov, A.F. Bloino, J. Zheng, G. Sonnenberg, J.L. Hada, M. Ehara, M. Toyota, K. Fukuda, R. Hasegawa, J. Ishida, M. Nakajima, T. Honda, Y. Kitao, O. Nakai, H. Vreven, T. Montgomery, Jr., J. A. Peralta, J. E. Ogliaro, F. Bearpark, M. Heyd, J.J. Brothers, E. Kudin, K.N. Staroverov, V.N. Kobayashi, R. Normand, J. Raghavachari, K. Rendell, A. Burant, J.C. Iyengar, S.S. Tomasi, J. Cossi, M. Rega, N. Millam, J.M. Klene, M.; Knox, J.E. Cross, J.B. Bakken, V. Adamo, C. Jaramillo, J. Gomperts, R. Stratmann, R.E. Yazyev, O. Austin, A.J. Cammi, R. Pomelli, C. Ochterski, J.W. Martin, R.L. Morokuma, K. Zakrzewski, V.G. Voth, G.A.; Salvador, P. Dannenberg, J.J. Dapprich, S. Daniels, A.D. Farkas, Ö. Foresman, J.B. Ortiz, J.V. Cioslowski, D.J. Fox, Gaussian, Inc., Wallingford CT, 2009.
[141] X.R. Yu, S.E. Levine, L.J. Broadbelt, Kinetic study of the copolymerization of methyl methacrylate and methyl acrylate using quantum chemistry, Macromolecules 41 (2008) 8242–8251.

[142] X.R. Yu, J. Pfaendtner, L.J. Broadbelt, Ab initio study of acrylate polymerization reactions: methyl methacrylate and methyl acrylate propagation, J. Phys. Chem. A 112 (2008) 6772–6782.
[143] M.W. Schmidt, et al., General atomic and molecular electronic-structure system, J. Comput. Chem. 14 (1993) 1347–1363.
[144] M.L. Coote, Computational quantum chemistry for free-radical polymerization, in: *third ed*., H.F. Mark (Ed.), Encyclopedia of Polymer Science and Technology, 9, *John Wiley & Sons*, *New York*, 2004, pp. 319–371.
[145] C. Eckart, The penetration of a potential barrier by electrons, Phys. Rev. 35 (1930) 1303.
[146] H. Eyring, The activated complex in chemical reactions, J. Chem. Phys. 3 (1935) 107–115.
[147] E. Wigner, Über Das Überschreiten Von Potentialschwellen Bei Chemischen Reaktionen, Z. Phys. Chem. 19 (1932) 203–216.
[148] I. Yavuz, G.A.A. Ciftcioglu, Dft characterization of the first step of methyl acrylate polymerization: performance of modern functionals in the complete basis limit, Comput. Theory Chem. 978 (2011) 88–97.
[149] C.Y. Lin, E.I. Izgorodina, M.L. Coote, First principles prediction of the propagation rate coefficients of acrylic and vinyl esters: are we there yet? Macromolecules 43 (2010) 553–560.
[150] R. Jain, T. Bally, P.R. Rablen, Calculating accurate proton chemical shifts of organic molecules with density functional methods and modest basis sets, J. Org. Chem. 74 (2009) 4017–4023.
[151] K.W. Wiitala, T.R. Hoye, C.J. Cramer, Hybrid density functional methods empirically optimized for the computation of C-13 and H-1 chemical shifts in chloroform solution, J. Chem. Theory Comput. 2 (2006) 1085–1092.
[152] K. Hori, T. Yamaguchi, K. Uezu, M. Sumimoto, A free-energy perturbation method based on monte carlo simulations using quantum mechanical calculations (Qm/Mc/Fep method): application to highly solvent-dependent reactions, J. Comput. Chem. 32 (2011) 778–786.
[153] S. Beuermann, Solvent influence on propagation kinetics in radical polymerizations studied by pulsed laser initiated polymerizations, Macromol. Rapid Commun. 30 (2009) 1066–1088.
[154] O.F. Olaj, I. Schnöll-Bitai, Solvent effects on the rate constant of chain propagation in free radical polymerization, Monat. Chem./Chem. Month. 130 (1999) 731–740.
[155] M. Cossi, V. Barone, B. Mennucci, J. Tomasi, Ab initio study of ionic solutions by a polarizable continuum dielectric model, Chem. Phys. Lett. 286 (1998) 253–260.
[156] I.A. Konstantinov, L.J. Broadbelt, Reaction free energies in organic solvents: comparing different quantum mechanical methods, Mol. Simul. 36 (2010) 1197–1207.
[157] P.N. Day, J.H. Jensen, M.S. Gordon, S.P. Webb, W.J. Stevens, M. Krauss, et al., An effective fragment method for modeling solvent effects in quantum mechanical calculations, J. Chem. Phys. 105 (1996) 1968–1986.
[158] M.S. Gordon, M.A. Freitag, P. Bandyopadhyay, J.H. Jensen, V. Kairys, W.J. Stevens, The effective fragment potential method: a Qm-based Mm approach to modeling environmental effects in chemistry, J. Phys. Chem. A 105 (2001) 293–307.
[159] A. Klamt, G. Schüürmann, Cosmo: a new approach to dielectric screening in solvents with explicit expressions for the screening energy and Its gradient, J. Chem. Soc. Perkin Trans. 2 (1993) 799–805.